Iowa State University
Digital Repository

Retrospective Theses and Dissertations

Iowa State University Capstones, Theses and Dissertations

1997

500mV low-voltage operational amplifier design

Jian Zhou
Iowa State University

Follow this and additional works at: https://lib.dr.iastate.edu/rtd

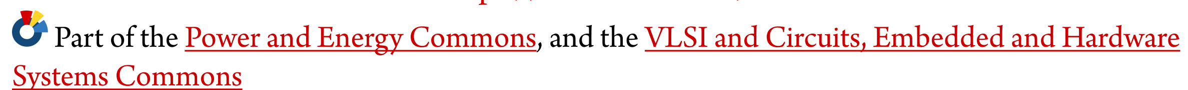
Part of the Power and Energy Commons, and the VLSI and Circuits, Embedded and Hardware Systems Commons

Recommended Citation
Zhou, Jian, "500mV low-voltage operational amplifier design" (1997). *Retrospective Theses and Dissertations*. 16751.
https://lib.dr.iastate.edu/rtd/16751

This Thesis is brought to you for free and open access by the Iowa State University Capstones, Theses and Dissertations at Iowa State University Digital Repository. It has been accepted for inclusion in Retrospective Theses and Dissertations by an authorized administrator of Iowa State University Digital Repository. For more information, please contact digirep@iastate.edu.

المنارة للاستشارات

www.manaraa.com

500mV low-voltage operational amplifier design

by

ISU
1997
Z545
c. 1

Jian Zhou

A thesis submitted to the graduate faculty
in partial fulfillment of the requirements for the degree of
MASTER OF SCIENCE

Major: Electrical Engineering
Major Professor: Randall Geiger

Iowa State University
Ames, Iowa
1997

Copyright © Jian Zhou, 1997. All rights reserved

المنارة للاستشارات
www.manaraa.com

Graduate College
Iowa State University

This is to certify that the Master's thesis of
Jian Zhou
has met the thesis requirement of Iowa State University

Signatures have been redacted for privacy

www.manaraa.com

TABLE OF CONTENTS

ACKNOWLEDGEMENTS ix

ABSTRACT x

CHAPTER 1. INTRODUCTION 1

1.1 Low voltage circuit design 1

1.2 Organization of the thesis 5

CHAPTER 2. MOSFET AND TWO STAGE OPERATIONAL AMPLIFIER DESIGN 7

2.1 Basic MOSFET operation 7

2.2 Small-signal model for MOSFETs 11

2.3 MOS transistor as a transmission gate 14

2.4 Two-stage operational amplifier design 15

CHAPTER 3. LOW-VOLTAGE OPERATIONAL AMPLIFIER DESIGN 19

3.1 Previous work 19

3.2 Threshold voltage tuning 21

3.3 Threshold tunable low-voltage operational amplifier 22

3.4 500mV operational amplifier design 23

3.5 DC voltage source 27

3.6 Simulation results 30

3.7 Conclusion 37

CHAPTER 4. SUPPLEMENTARY CIRCUIT IMPLEMENTATIONS 39

4.1 Supplementary circuits 39

4.2 Reference voltage generation 40

4.3 High voltage and negative voltage generator 47

للاستشارات

www.manaraa.com

4.4 Oscillator 50
4.5 Nonoverlapping clocks 54
4.6 Pulse generator 56
4.7 Conclusion 56
CHAPTER 5: CONCLUSIONS 58
APPENDIX A: LEVEL 3 HSPICE MODEL 60
APPENDIX B: LEVEL 13 HSPICE MODEL 61
APPENDIX C: NETLIST FOR THE CIRCUIT SIMULATION 63
BIBIOGRAPHY 73

المنارة للاستشارات
www.manaraa.com

LIST OF FIGURES

Figure 1.1	Supply voltage scaling	2
Figure 1.2	Power supply and power dissipation in previous work	5
Figure 2.1	(a) Structure of an nMOSFET and a pMOSFET (b) Top view of the nMOSFET and pMOSFET	8
Figure 2.2	MOSFET operational structure	9
Figure 2.3	Output characteristic of the nMOSFET	11
Figure 2.4	Small-signal model of the MOSFET	12
Figure 2.5	Simplified small-signal model for the MOSFET	13
Figure 2.6	(a)nMOS transistor as a transmission gate (b)Transfer characteristics of an nMOS pass transistor	14
Figure 2.7	(a)pMOS transistor as a transmission gate (b)Transfer characteristics of a pMOS pass transistor	15
Figure 2.8	Schematic of a two-stage operational amplifier	16
Figure 3.1	Complementary differential input stage	19
Figure 3.2	Floating gate MOS transistor cell	19
Figure 3.3	Threshold voltage tunable structure	21
Figure 3.4	Threshold voltage tuning effects	22
Figure 3.5	Threshold tunable low-voltage operational amplifier	22
Figure 3.6	Frequency response of the original two-stage operational amplifier (a) Magnitude response (b) Phase response	25
Figure 3.7	Frequency response of the proposed 500mV low voltage operational amplifier. (a) Magnitude response (b) Phase response	26
Figure 3.8	DC voltage source (a) Symbol (b) Circuit implementation	27
Figure 3.9	DC effects in the switched capacitor circuits	28
Figure 3.10	Waveform for ϕ_1 and ϕ_2	28

المنارة للاستشارات
www.manaraa.com

Figure 3.11	Small-signal model considering the capacitor effects	29
Figure 3.12	Leakage current effects and discharge circuit	30
Figure 3.13	Simulation circuit for the switched capacitor	31
Figure 3.14	Frequency response of the 500mV low voltage operational amplifier (a) Magnitude response (b) Phase response	32
Figure 3.15	(a) Test circuit for unity gain DC transfer characteristics (b) Test circuit for unity gain step response	34
Figure 3.16	(a) Unity gain DC transfer characteristics of the 3.3V operational amplifier (b) Unity gain DC transfer characteristic of the 500mV operational amplifier	35
Figure 3.17	(a) Unity gain step response of the 3.3V operational amplifier (b) Unity gain step response of the 500mV operational amplifier	36
Figure 3.18	Layout of the 500mV low-voltage operational amplifier core	38
Figure 4.1	Low-voltage operational amplifier architecture	39
Figure 4.2	Threshold voltage variation effects	40
Figure 4.3	Threshold voltage extraction	41
Figure 4.4	Block diagram and circuit of an attenuator consisting of two nMOSFETs	42
Figure 4.5	DC transfer characteristic of the attenuator consisting of two nMOSFETs	43
Figure 4.6	Block diagram and circuit of an attenuator consisting of two pMOSFETs	44
Figure 4.7	DC transfer characteristic of the attenuator consisting of two pMOSFETs	45
Figure 4.8	DC reference voltage generator for Approach 1	46
Figure 4.9	DC reference voltage generator for Approach 2	47
Figure 4.10	(a)Charge pump circuit (b)Clock waveforms	48
Figure 4.11	Simulation results for the charge pump	49
Figure 4.12	Negative substrate voltage generator	49
Figure 4.13	Simulation result for the negative voltage generator	50
Figure 4.14	Ring oscillator	51

المنارة للاستشارات

www.manaraa.com

Figure 4.15	Cross section and top view of the floating gate transistor	52
Figure 4.16	A simplified capacitive equivalent circuit of the floating transistor	53
Figure 4.17	Circuit configuration of the bootstrapped buffer	54
Figure 4.18	Simulation results of the bootstrapped buffer	55
Figure 4.19	Nonoverlapping clock (a) Clock signals (b) Circuit implementation	55
Figure 4.20	Shift register as a pulse generator	56

المنارة للاستشارات

www.manaraa.com

LIST OF TABLES

Table 1.1	Low-voltage operational amplifier characteristics and techniques been used	4
Table 3.1	Device sizes used in the two-stage operational amplifier	22
Table 3.2	Simulated frequency response of the 500mV low-voltage operational amplifier	31
Table 3.3	Comparisons of performance parameters of the two operational amplifiers	34
Table 4.1	Power dissipation in the low-voltage operational amplifier circuits	54

المنارة للاستشارات

www.manaraa.com

ACKNOWLEDGEMENTS

I would like to express my heartful appreciation to my major professor Dr. Randall L. Geiger. I wish to thank him for his guidance, support and help throughout my master program at Iowa State University. He introduced me to the challenging and exciting Mixed-Signal and Analog VLSI field throughout his great course and research guidance. He is always there ready for help whenever I have questions. His academic excellence and foresight have been of great help to me and have had an important effect on my life.

I would also like to express my thanks to my co-major professor Dr. Marwan Hassoun. He brought me to Iowa State University and gave me a lot of encouragement. I would like to express my appreciation to Dr. E. K. F. Lee for his constructive comments and suggestions on the circuit implementation. I wish to acknowledge Dr. William Black for his great course and instructions on the layout for the research project. I would also like to thank Dr. David Kao for his time serving as my committee member.

Throughout my masters program, my colleagues gave me a lot of help, which made my life enjoyable and productive. I would like to thank Huawen Jin for his suggestions during various discussions which were of great help to my work. I would also like to thank Xiaohong Du, Lin Wu and Yiqing Chen for being my course partners; we really shared a lot of things together.

Lastly, I would like to thank my wife, parents and sisters for their endless love and support in every respect.

المنارة للاستشارات

www.manaraa.com

ABSTRACT

With the dramatic increase in the number of transistors on a chip and the increasing needs for battery-powered applications, low-voltage circuit design techniques have been widely studied in recent year. However, these low supply voltage research efforts have been focused mainly on digital circuits, especially on high density memory circuits. Reported success in achieved high performance low voltage operation in analog circuits lags far behind. Recent results have been presented on CMOS low-voltage operational amplifiers, where the supply voltage has been reduced to less than 2.5V in which the complementary input stages were used to keep the g_m constant [SI95] [HL85]. Recently, the floating gate MOS transistor has attracted considerable interest as a nonvolatile analog storage device and as a precision analog trim element because it has threshold voltage programming ability [YU93] [RC95].

The particular focus of this work is on implementing very low voltage analog and mixed-signal integrated circuit in a standard CMOS process. As a proof-of-concept vehicle, this work concentrates on the design of very low voltage operational amplifiers in standard CMOS processes. By connecting a DC reference voltage source in series with the gate of all MOS transistors, the equivalent threshold voltage of all transistors can be electrically lowered. This technique makes it possible to decrease the power supply voltage. The DC reference voltage sources are realized by using a switched capacitor charged periodically and switched between the actual circuit and a reference precharge circuit. By extracting the reference voltage source directly from the threshold voltage itself, the threshold voltage variations due to the process and temperature variations can be compensated, since large threshold variations are intolerable for very low threshold voltage applications. In a proof-of-concept two-stage operational amplifier designed to operate with a single 500mV power supply in a standard 2μ process, the tail current is kept the same as in a 3.3V design, thus the key performance parameters are expected to

www.manaraa.com

be maintained at reasonable values. The dramatic decrease of the power supply possible with this approach is paralleled with a corresponding reduction in the power dissipation. Simulation results of this 500mV operational amplifier show a 70dB DC gain, 7.8MHz unity gain bandwidth and a 65° phase margin. Power dissipation is reduced by more than 90% from that of the corresponding 3.3V design.

Although the specific implementation is focused on the implementation of an operational amplifier with comparable performance parameters to those with larger supply voltage, the dominant applications of this technique are for designing a variety of analog and mixed-signal systems that operate at very low voltages and with low power dissipation.

المنارة للاستشارات

www.manaraa.com

CHAPTER 1. INTRODUCTION

This chapter gives the motivation behind this thesis work. The questions of why low-voltage circuit design is important and why low-voltage operational amplifiers are needed are answered. The chapter is concluded with a summary of the organization of this thesis.

1.1 Low-voltage circuit design

During the past two decades, low supply voltage and low-power circuit design techniques have attracted more and more interests and have been widely studied. The motivation behind low-voltage and low-power circuit design is primarily due to three reasons.

The first reason arises from constant reduction of the minimum feature size (i.e. minimum gate length) of a MOS transistor. As the minimum channel length has been scaled down to submicron levels, the gate oxide thickness has been reduced to several nanometers. With the decreasing thickness of gate oxide, the electric field strength in the gate oxide for a fixed supply voltage increases sharply. To avoid gate breakdown and ensure device reliability, the supply voltage has to be reduced. For the 5 micron to 2 micron range, 5V supply voltage is widely used. Currently, 1.2 micron and 0.5 micron processes use 3.3V to 2.5V supply voltages. It is expected that when minimum feature sizes are scaled down to deep submicron levels, acceptable supply voltage will be 2.2V or lower. This trend is illustrated in Figure 1.1.

The second reason emanates from the increasing density of components on chip. With the increasing number of components integrated on a chip, more power will be dissipated on chip if the same voltage and current levels are maintained. For example, Pentium II has 7.5 million transistors on chip and dissipates 43 Watts. Such high power

المنارة للاستشارات
www.manaraa.com

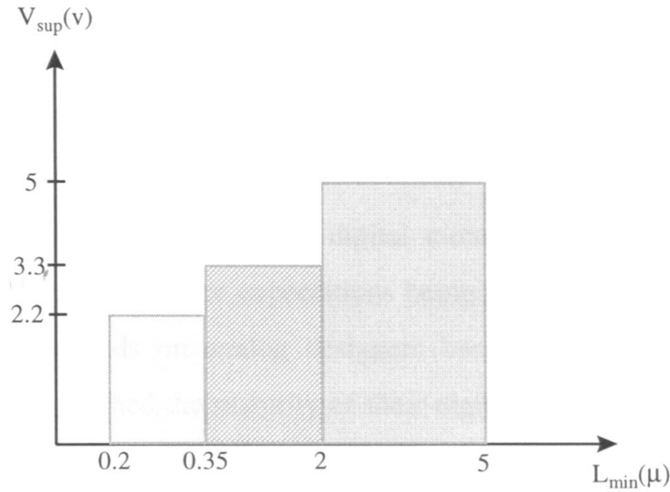

Figure 1.1 Supply voltage scaling

dissipated on chip will cause serious overheating problem of the chip. Reducing the supply voltage can help to prevent the overheating problem.

The third reason is due to the increasing demand for battery-powered applications. In order to have an acceptable operation period from a battery, the supply power must be as small as possible.

Motivated by a reduction of power dissipation and reduction of supply voltage, considerable research has been carried out on reducing supply voltage and power dissipation in digital circuits, especially on high density memory circuits such as DRAMs and SRAMs [MA96], [KT96]. The low-voltage low-power digital circuits attain good performance qualities such as high accuracy and a large signal-to-noise ratio that parallels the dramatic reduction of the size of the digital part due to the decrease of feature sizes. Total power dissipation of the digital circuits can be expressed as [WE93]

$$P_{total} = P_S + P_D + P_{SC} \tag{1.1}$$

where P_S represents the static power dissipation, P_D represents the dynamic power dissipation and P_{SC} represents short circuit power dissipation. For a complex circuit and high frequency applications, the dynamic power will dominate, thus

$$P_{total} \approx P_D = C_{load} \cdot V_{DD}^{\ 2} \cdot f_p \tag{1.2}$$

المنارة للاستشارات
www.manaraa.com

where C_{load} is the total load capacitance and f_p is the operation frequency.

Equation (1.2) shows that the power dissipation is quadratically dependent on the supply voltage V_{DD}. Potential power reduction can be achieved by lowing the supply voltage.

Paralleling the increasing role of digital circuits in current signal processing systems are increasing performance expectations being placed on analog circuits. This is placing increasing demands on analog designers because the computer-aided analog design tools have not reached the maturity of their digital counterparts. The necessity of building these high performance analog circuits becomes apparent by observing that living in a real world, the signals to and from devices such as the sensors and actuators which communicate with the outside world, are inherently analog. In order to keep pace with the developments in digital circuit design, low-voltage low-power analog circuit design becomes critical.

Low-voltage operation is being paralleled with the scaling of threshold voltages. One of the most challenging difficulties imposed with the scaling of threshold voltages is the increased relative threshold voltage variation. Threshold voltage scaling requires complicated technology known as "substrate engineering" and the costs associated with developing new and specialized processes that are sufficiently stable to support high voltage commercial production are enormous. A new method to electrically lower the threshold voltage while still maintaining a standard process will be presented in this work.

One of the most important analog building blocks is the operational amplifier. It has found its way into numerous applications, such as switched capacitor filters, active filters, charge amplifiers, data converters and more. The design of high performance low-voltage low-power operational amplifiers is one of the most challenging areas facing analog circuit designers today. Many papers and books have been published on this subject [HH96], [SI95].

A technique for dramatically reducing the power supply voltage for analog and mixed-signal circuits will be introduced in this thesis. As a "proof of concept" for

المنارة للاستشارات
www.manaraa.com

employing this technique, a very-low-voltage operational amplifier will be designed. Although the major emphasis in this is on the design of the operational amplifier, the major contribution is in establishing that this basic approach to very-low-voltage design is possible.

Low-voltage operational amplifier design can be divided into three groups, low-voltage, very-low-voltage and ultra-low-voltage. Operational amplifiers in the first group can operate on supply voltages between 2V and 5V. At the lower end of this range, this corresponds to about two stacked gate-source voltages and two stacked saturation voltages. Operational amplifiers in the second group have supply voltages between 1V and 2V and typically provide the designer with only one gate-source voltage and one saturation voltage. Operational amplifiers in the third group operate on supply voltages below 1V. There is little literature available in the ultra-low voltage range.

Most of previous work on low-voltage operational amplifier design belonged to the previous two groups. Table 1.1 summarizes some previous work in the area and the performance parameters they achieved.

Table 1.1: Low-voltage operational amplifier characteristics and techniques been used

	V_{DD}-V_{SS}	Gain (dB)	Pdiss (W)	Year	Technique
Eggermont [EC96]	2	65	100μ	1996	SOI CMOS & $g_{mn}+g_{mp}$
Huijsing [HL85]	1.5	100	0.3m	1985	BiCMOS & $g_{mn}+g_{mp}$
Fonderie [FM89]	1	100	10m	1989	BiCMOS & $g_{mn}+g_{mp}$
Huang [HC97]	1.5	100	0.89m	1997	BiCMOS & $g_{mn}+g_{mp}$
Sakurai [SI96]	2.5	80	~1m	1996	$g_{mn}+g_{mp}$
Allen [AB95]	1	>50	45μ	1995	Bulk driven MOSFET
Angulo [AC95]	1.5	N/A	N/A	1995	Floating gate

Figure 1.2 illustrates the power supply voltage and power dissipation achieved in the previous work. We can see that the power supply voltage in all previous work was higher than 1V. No one has been successful at pushing the supply voltage down to lower than 1V. It can be further observed that progress in power supply voltage scaling has slowed as designers approached the 1V hurdle with 100mV decreases in power supply

المنارة للاستشارات
www.manaraa.com

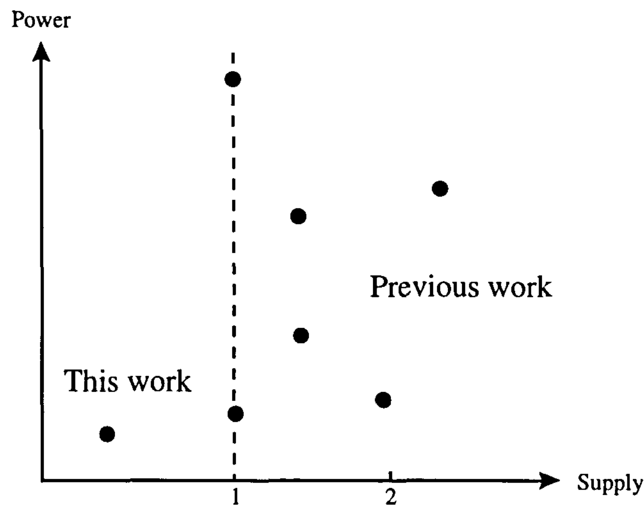

Figure 1.2 Power supply and power dissipation in previous work

voltage being viewed as significant contributions. For the low supply voltage work referenced, all approaches either utilized complementary input stages or utilized specialized processes that are not widely available for commercial production.

This thesis presents a new method for designing ultra low-voltage operational amplifiers. Some of the merits are list below:

- Utilizes existing standard process
- Ultra low supply voltage-0.5V
- Comparable key performance parameters to high-voltage designs
- Low power dissipation

1.2 Organization of the thesis

The main focus of this thesis will be to design a very low-voltage operational amplifiers. Following this introduction, Chapter 2 will describe some general background on MOSFETs and the design of operational amplifiers. Chapter 3 gives a literature review on low-voltage operational amplifier design. This is followed by a discussion of the proposed ultra low-voltage operational amplifier. In this chapter, design considerations will be explained in detail. Chapter 4 provides the supplementary circuits that support the

المنارة للاستشارات
www.manaraa.com

ultra low-voltage operational amplifier. The threshold voltage variation compensation technique is also described in more detail. Finally, Chapter 5 addresses conclusions and future work on this topic.

المنارة للاستشارات
www.manaraa.com

CHAPTER 2. MOSFET AND TWO-STAGE OPERATIONAL AMPLIFIER DESIGN

Before I start a discussion of the proposed operational amplifier structure, some basic details regarding MOSFET operation will be given. The design procedure of a two-stage operational amplifier will follow.

2.1 Basic MOSFET operation

CMOS technology is widely used for designing integrated circuits over Bipolar and MESFET technology due to the advantages such as greater density and simpler process technology. CMOS technology provides two types of transistors, an n-type transistor (nMOS) and a p-type transistor (pMOS) where electrons and holes provide the conduction mechanisms respectively. Figure 2.1 shows the typical physical structures for the two types of MOS transistors. For the nMOS transistor, the lightly doped p^- material is called the substrate or bulk. The two heavily doped p^+ regions diffused in the substrate are called the drain and source regions respectively and are separated by a distance of L (referred to as the device length). At the surface between the drain and the source lies a gate electrode that is separated from the silicon by a thin dielectric material. Similarly, the pMOS transistor is formed by two heavily doped p^+ regions separating the lightly doped n^- well with a gate bridging the drain and the source.

The MOSFET is fundamentally a voltage controlled current source with the controlling voltage applied between the gate and the source. The basic operation of MOS transistors will be for an nMOS transistor. The basic operation of a pMOS transistor is the same. In Figure 2.2(a), we show an nMOS transistor where the source and the substrate are grounded and the drain and the gate are tied to separate voltages. Based

المنارة للاستشارات

www.manaraa.com

upon the different values of V_{GS} and V_{DS}, the nMOS transistor will operate in three different regions: cutoff region, ohmic region and saturation region.

Cutoff Region: If V_{GS} is smaller than a certain voltage, no current will flow through the transistor and the transistor is said to be in cutoff region. In the cutoff region, the transistor acts like a open circuit and the drain current, I_D, is zero.

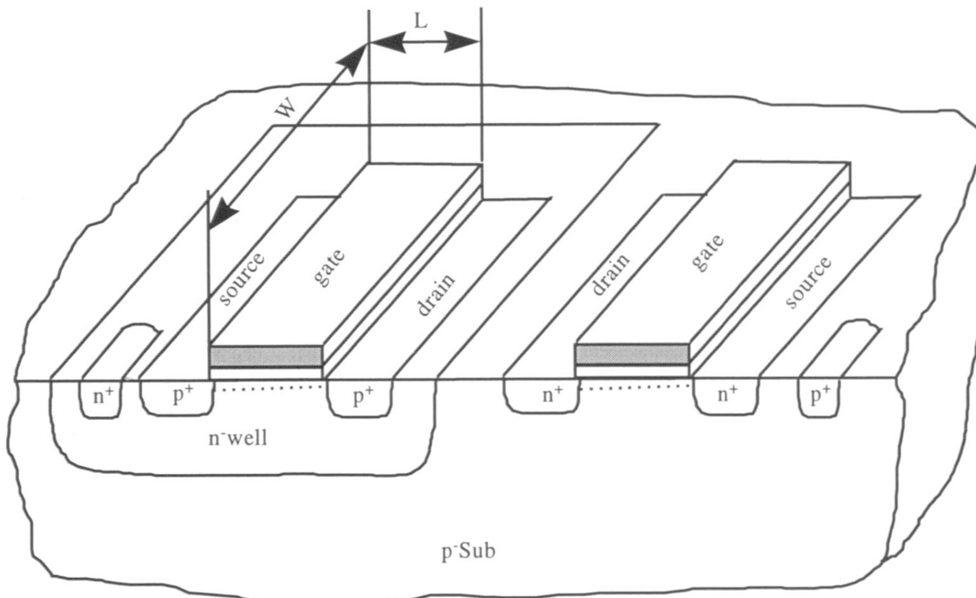

(a)

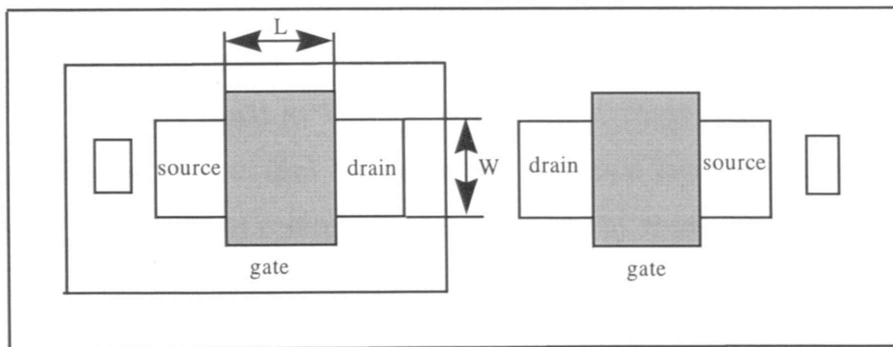

(b)

Figure 2.1 (a) Structure of an nMOSFET and a pMOSFET

(b) Top view of the nMOSFET and pMOSFET

المنارة للاستشارات
www.manaraa.com

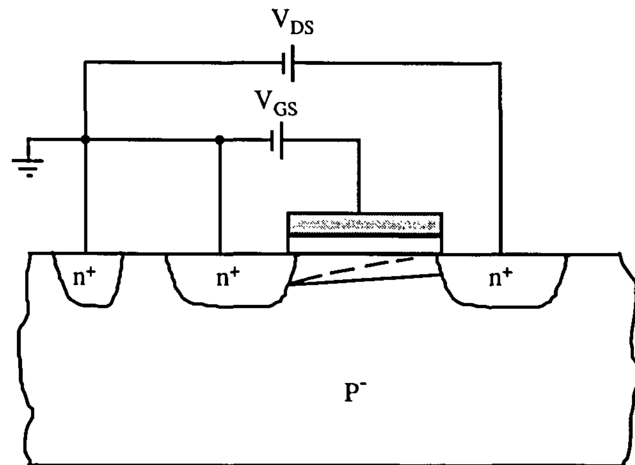

Figure 2.2 MOSFET operation structure

Ohmic Region: If V_{GS} is increased, an inversion of the p-type semiconductor materials under the gate will occur by attracting electrons to the surface of this region under the gate. The region where the inversion takes place is called the channel and the voltage, V_{GS}, necessary to create the inversion layer is called the threshold voltage, V_T. If V_{DS} is sufficiently small, the inversion region exists everywhere between the drain and the source. In this region, the nMOS transistor is said to be in the ohmic (or triode) region. In the ohmic region, the transistor acts like a voltage controlled resistor, whereby the resistance between the drain and source is controlled by V_{GS}.

Saturation Region: If V_{DS} is increased, the drain current will also keep increasing until V_{DS} becomes equal to V_{GS}-V_T. When V_{DS} is larger than V_{GS}-V_T, the gate drain voltage V_{GD} is smaller than V_T hence the inversion layer at the drain end starts to disappear and the drain current will not increase any more with increased V_{DS}. At this point, the drain current is independent of V_{DS}. At this point, the transistor is said to be operating in saturation region.

A summary of the MOSFET model for both n-channel and p-channel devices is given as follows:

المنارة للاستشارات
www.manaraa.com

nMOS transistor

$$I_D = \begin{cases} 0 & V_{GS} < V_T,\ V_{DS} \geq 0 \ \text{(cutoff)} \\ \dfrac{\mu_n \cdot C_{ox} \cdot W}{L}\left(V_{GS} - V_T - \dfrac{V_{DS}}{2}\right) \cdot V_{DS}\left(1 + \lambda \cdot V_{DS}\right) & V_{GS} > V_T,\ 0 < V_{DS} < V_{GS} - V_T \text{(ohmic)} \\ \dfrac{\mu_n \cdot C_{ox} \cdot W}{2 \cdot L}\left(V_{GS} - V_T\right)^2 \cdot \left(1 + \lambda \cdot V_{DS}\right) & V_{GS} > V_T,\ V_{DS} > V_{GS} - V_T \text{(saturation)} \end{cases}$$

(2.1)

where,

$$V_T = V_{T0} + \gamma.(\sqrt{\phi - V_{BS}} - \sqrt{\phi})$$

pMOS transistor

$$I_D = \begin{cases} 0 & V_{GS} > V_T,\ V_{DS} \geq 0 \ \text{(cutoff)} \\ -\dfrac{\mu_p \cdot C_{ox} \cdot W}{L}\left(V_{GS} - V_T - \dfrac{V_{DS}}{2}\right) \cdot V_{DS}\left(1 - \lambda \cdot V_{DS}\right) & V_{GS} < V_T,\ 0 > V_{DS} > V_{GS} - V_T \text{(ohmic)} \\ -\dfrac{\mu_p \cdot C_{ox} \cdot W}{2 \cdot L}\left(V_{GS} - V_T\right)^2 \cdot \left(1 - \lambda \cdot V_{DS}\right) & V_{GS} < V_T,\ V_{DS} < V_{GS} - V_T \text{(saturation)} \end{cases}$$

(2.2)

where,

$$V_T = V_{T0} + \gamma.(\sqrt{\phi - V_{BS}} - \sqrt{\phi})$$

The various parameters used in above equation are defined as

μ_n = surface mobility of the channel for the nMOS transistor

μ_p = surface mobility of the channel for the pMOS transistor

C_{ox} = capacitance per unit area of the gate oxide

W = effective channel width

L = effective channel length

λ = channel length modulation parameter

γ = bulk threshold parameter

ϕ = strong inversion surface potential

The output characteristics of the MOS transistor can be developed from the above equations. Figure 2.3 shows these characteristics. The solid line in the figure corresponds

المنارة للاستشارات

www.manaraa.com

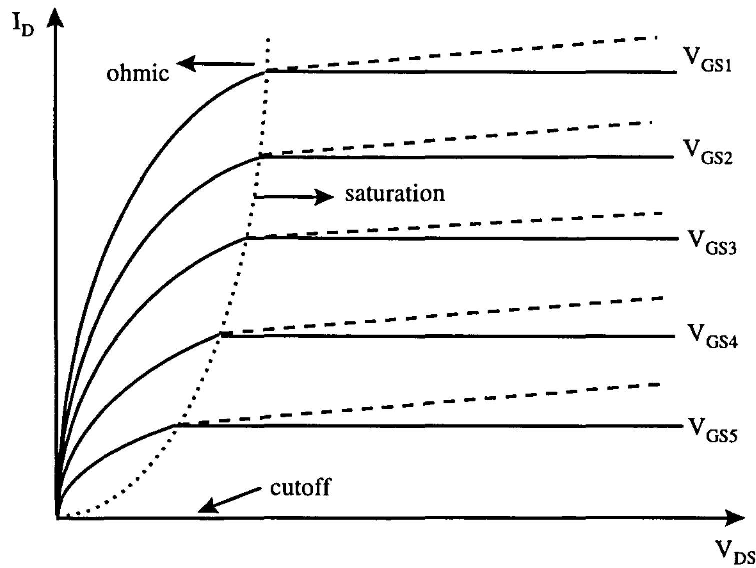

Figure 2.3 Output characteristics of the nMOSFET

to the output characteristics when no channel length modulation is considered while dotted lines reflect operation of the actual device in which channel length modulation effects are included.

2.2 Small-signal model for MOSFETs

In the preceding section, the MOS large signal model was discussed. In order to evaluate the response of gain stages to small signals, a small-signal model of the transistors must be used. Small signal parameters are defined in terms of the ratio of small perturbations of the large signal variables or as the partial differentiation of one large-signal variable with respect to another.

Figure 2.4 shows a linearized small-signal model for the MOS transistor [AH87]. Since the small-signal parameters are all related to the large-signal parameters and dc variables, they can be obtained directly from the dc model and model parameters summarized in the preceding section.

$$g_m = \left. \frac{\partial I_D}{\partial V_{GS}} \right|_Q \quad (2.3)$$

المنارة للاستشارات
www.manaraa.com

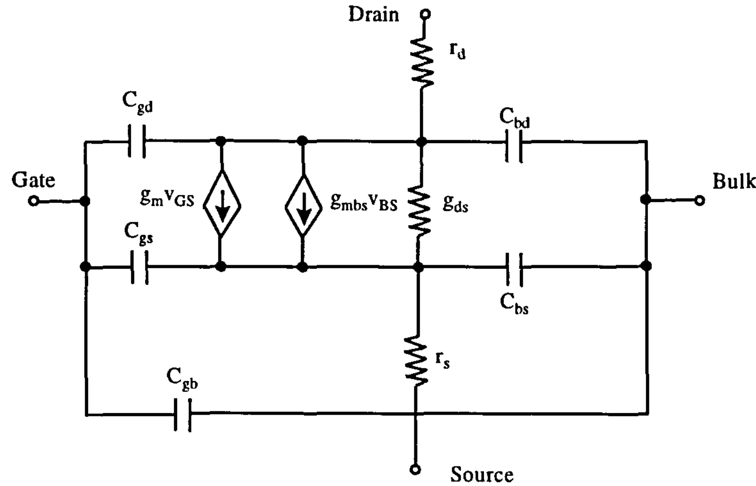

Figure 2.4 Small-signal model of the MOSFET

$$g_{mbs} = \left. \frac{\partial I_D}{\partial V_{BS}} \right|_Q \tag{2.4}$$

$$g_{ds} = \left. \frac{\partial I_D}{\partial V_{DS}} \right|_Q \tag{2.5}$$

Since there are three regions of operation in the dc large-signal model, there are three different small-signal models corresponding to each of these three different regions. The model given above can be simplified according to different operation regions and specific requirements.

Cutoff Region: Since in the cutoff region, the drain current is essentially zero, the MOSFET works only as a passive component consisting of some capacitive components. All three of the transconductor parameters are essentially zero.

Ohmic Region: The MOS transistor is seldom used as a three terminal device when operating in the ohmic region. Ohmic region operation is common when the gate voltage is fixed at a constant DC value. In this situation, the MOSFET behaves as a resistor between drain and source and the resistance is voltage-controllable by the DC value of V_{GS}. The ohmic region resistance can be obtained from the equation

$$I_D = \frac{\mu_n \cdot C_{ox} \cdot W}{L}\left(V_{GS} - V_T - \frac{V_{DS}}{2}\right) \cdot V_{DS}\left(1 + \lambda \cdot V_{DS}\right)$$

www.manaraa.com

neglecting the λ effect, we obtain the resistance

$$R_{FET} = \frac{I_D}{V_{DS}} = \mu_n \cdot C_{ox} \cdot \left(\frac{W}{L}\right) \cdot \left(V_{GS} - V_T - V_{DS}\right) \quad (2.6)$$

For the case V_{ds} is very close to zero,

$$R_{FET} = \mu_n \cdot C_{ox} \cdot \left(\frac{W}{L}\right) \cdot \left(V_{GS} - V_T\right) \quad (2.7)$$

The MOSFET normally will not be biased in the ohmic region due to the performance limitation.

Saturation Region: For most of applications, the MOS transistor is biased in the saturation region. In the saturation region, the small-signal parameters can be drived as follows: using equation (2.1), the large-signal model current, I_D, in saturation region is:

$$I_D = \frac{\mu_n \cdot C_{ox} \cdot W}{2 \cdot L} \left(V_{GS} - V_T\right)^2 \cdot \left(1 + \lambda \cdot V_{DS}\right)$$

hence, the nonzero parameters are:

$$g_m = \left.\frac{\partial I_D}{\partial V_{GS}}\right|_Q = \frac{\mu_n \cdot C_{ox} \cdot W}{L} \cdot \left(V_{GS} - V_T\right) \cdot \left(1 + \lambda \cdot V_{DS}\right) \approx \sqrt{2 \cdot \frac{\mu_n \cdot C_{ox} \cdot W}{L} \cdot I_{DQ}} \quad (2.8)$$

$$g_{mbs} = \left.\frac{\partial I_D}{\partial V_{BS}}\right|_Q = \eta \cdot g_m \quad (2.9)$$

$$g_{ds} = \left.\frac{\partial I_D}{\partial V_{DS}}\right|_Q = \lambda \cdot \left|I_{DQ}\right| \quad (2.10)$$

The small-signal model is shown in Figure 2.5. Since the current $g_m \cdot v_{GS}$ typically

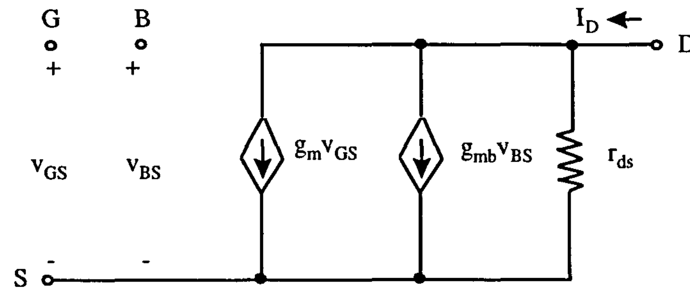

Figure 2.5 Simplified small-signal model for the nMOSFET

المنارة للاستشارات
www.manaraa.com

will dominate the drain current, the small-signal MOS transistor is inherently a good transconductance amplifier [GA90].

2.3 MOS transistor as a transmission gate

MOS transistors are often used as transmission gates. An nMOS pass transistor is depicted in Figure 2.6(a). The operation of the MOS pass transistor can be explained by considering the charging and discharging of the load capacitor through the MOS pass transistor. Assume initially that the load capacitor is discharged and the gate voltage is 0. At the time point t_1, the gate voltage becomes a positive voltage V_G ($V_G>V_T$). Since V_{GS} is greater than V_T, there will be current flowing through the nMOS transistor from the input to the output. As the output voltage increases, V_{GS} becomes small. If V_{in} is greater than $V_G - V_T$, when the output approaches $V_{out} = V_G - V_T$, the nMOS transistor begins to turn off. Thus the output will keep constant value at $V_G - V_T$. If V_{in} is smaller than $V_G - V_T$ it can be transferred directly to the output. The transfer characteristics are illustrated in Figure 2.6(b).

The operation of a pMOS transistor is different from an nMOS transistor. Referring to Figure 2.7(a), assume initially the load capacitor is discharged and the gate

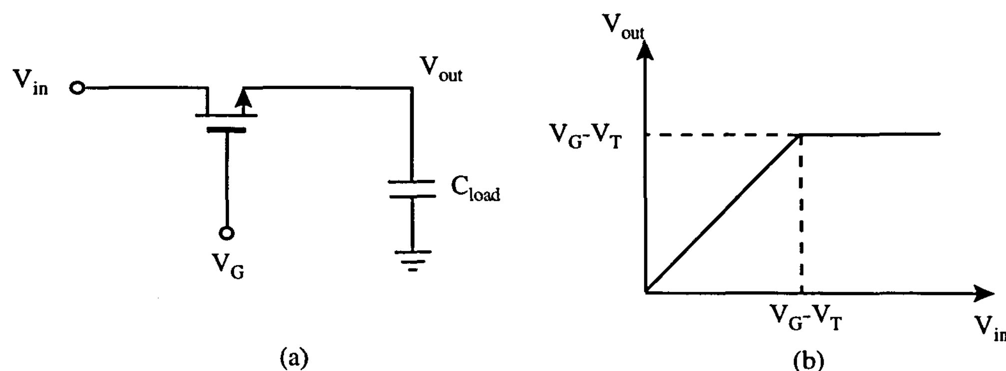

Figure 2.6 (a) nMOS transistor as a transmission gate

(b) Transfer characteristics of an nMOS pass transistor

المنارة للاستشارات

www.manaraa.com

voltage is high. At the time point t_1, V_G becomes low and a high voltage source is applied to V_{in}. Since $V_{GS} < V_T$ now, there will be current flowing from the input to the output until the output reaches V_{in}. Now, if we connect V_{in} to GND, the load capacitor will discharge through the pMOS transistor. However, when V_{out} approaches V_T, $V_{GS} > V_T$, the pMOS transistor will cutoff. The transfer function of a pMOS pass transistor is illustrated in Figure 2.7(b).

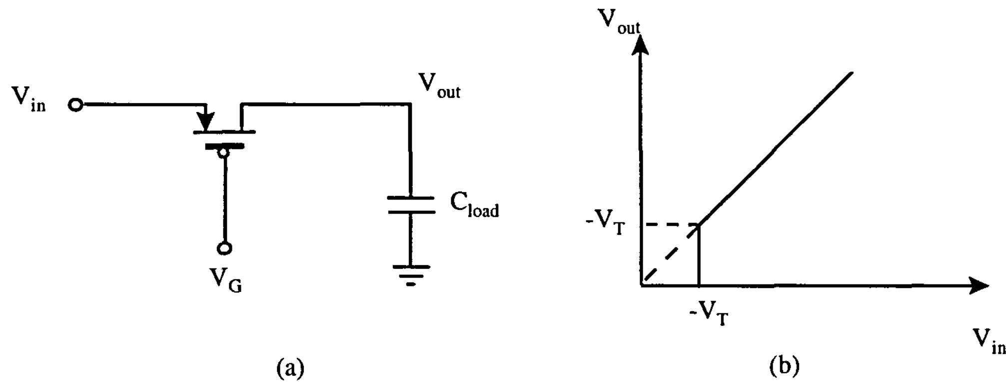

Figure 2.7 (a) pMOS transistor as a transmission gate

(b)Transfer characteristics of a pMOS pass transistor

2.4 Two-stage operational amplifier design

The operational amplifier is one of the most important building blocks in analog circuits design. Among the versatile operational amplifier structures, the two-stage operational amplifier is very common because it can provide relatively high gain and with the appropriate feedback compensation, it can meet the stability requirement. In this section, a procedure for designing the two-stage operational amplifier will be reviewed. Figure 2.6 shows a typical two-stage operational amplifier. Some important relationships describing the operational amplifier performance are summarized as follows [AH87]:

Slew rate $$SR = \frac{I_5}{C_C} \quad (2.11)$$

First stage gain $$A_{v1} = \frac{V_{o1}}{V_d} = \frac{V_{o1}}{V_+ - V_-} = \frac{g_{m2}}{g_{ds2} + g_{ds4}} = \frac{2g_{m2}}{I_5 \cdot (\lambda_2 + \lambda_4)} \quad (2.12)$$

المنارة للاستشارات
www.manaraa.com

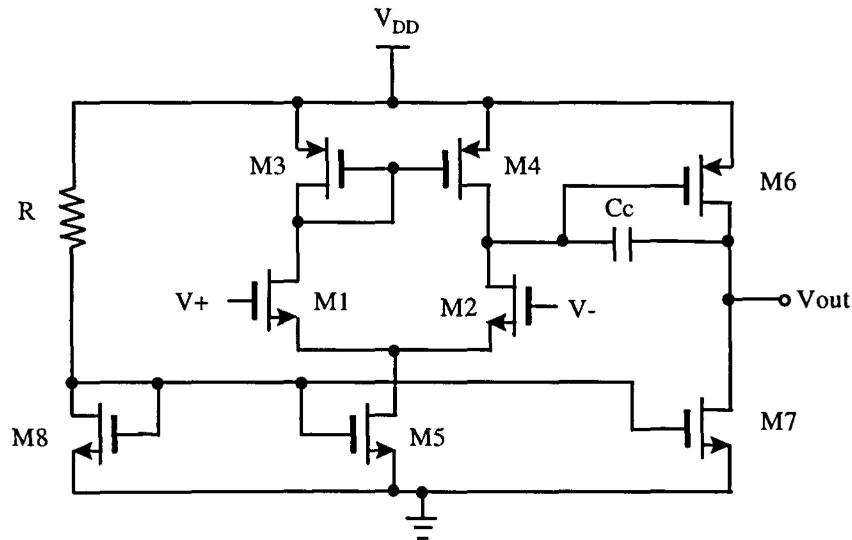

Figure 2.8 Schematic of a two-stage operational amplifier

Second stage gain $$A_{v2} = \frac{V_{out}}{V_{o1}} = \frac{g_{m6}}{g_{ds6} + g_{ds7}} = \frac{g_{m6}}{I_6 \cdot (\lambda_6 + \lambda_7)} \quad (2.13)$$

Gain-bandwidth $$GB = \frac{g_{m2}}{C_C} \quad (2.14)$$

Although different applications will require different performance of the operation amplifiers, some common specifications are of specific interests for most of the operational amplifiers.

1. DC gain A_v
1. Gain-bandwidth product, GB
2. Maximum load capacitance, C_L
3. Slew-rate, SR
4. Input common-mode range, CMR
5. Output voltage swing
6. Power dissipation, P_{diss}

A procedure for designing a two-stage operational amplifier follows. The first design step is to choose a device length to be used throughout the circuit. This value will

المنارة للاستشارات

www.manaraa.com

determine the value of channel length modulation parameter λ, which is a critical parameter in the calculation of the amplifier gain.

The next design step is to determine the value of the compensation capacitor C_c. It was known that in two pole systems, in order to obtain a 60° phase margin, the second pole has to be beyond 2.2 times of the unit gain bandwidth GB. It was shown that such pole requirement will result in the minimum value for the compensation capacitor [AH87].

$$Cc \geq 0.22 \cdot C_L \tag{2.15}$$

For the certain application, C_L is known, hence the compensation capacitor can be easily obtained.

The following step in the design is to determine the tail current I_5. From the equation (2.13), we can see that the tail current can be obtained based upon the knowledge of compensation capacitor C_c and slew rate requirement,

$$I_5 = SR(slewrate) \cdot C_c \tag{2.16}$$

The tail current is mirrored from the current mirror consisting of transistor M_5 andM_8, assume the size of the two transistors are same, the drain current of transistor M8 is known, acccordingly, the value of the resistor R can be obtained.

$$R \approx \frac{V_{DD} - V_{dsatM8}}{I_5} \tag{2.17}$$

The size of the M_2 can be determined by using the requirement for the unit gain bandwidth.

$$GB = \frac{g_{m2}}{C_C} \tag{2.18}$$

$$g_{m2} = \sqrt{2\mu \cdot C_{ox} \cdot I_{DS2} \cdot \left(\frac{W}{L}\right)_2} \tag{2.19}$$

With C_C and $I_{DS2} = {I_{DS5}}/{2}$ available, solving the above equations gives the ratio of $\left({W}/{L}\right)_2$. Since M1 and M2 are matched, $\left({W}/{L}\right)_1$ is also obtained.

المنارة للاستشارات

www.manaraa.com

In order to make the zero due to the Miller compensation larger than the second pole, we choose $I_{DS6} = I_{DS7} = 5 \cdot I_{DS2} = 5 \cdot I_{DS1}$, since $I_{DS1} = I_{DS2} = {I_{DS5}}/{2}$, we can easily obtain the size of the M7.

$$\frac{\left(W/L\right)_7}{\left(W/L\right)_5} = \frac{I_{DS7}}{I_{DS5}} \tag{2.20}$$

Using the equation for the DC gain

$$A_v = A_{v1} \cdot A_{v2} = \frac{2g_{m2}}{I_5 \cdot \left(\lambda_2 + \lambda_4\right)} \cdot \frac{g_{m6}}{I_6 \cdot \left(\lambda_6 + \lambda_7\right)} \tag{2.21}$$

we can solve the size of M_6 since we have all of other parameters used in this equation.

The final parameter to be solved is the size of M_3 and M_4. If we force the V_{GS3} to be equal to V_{GS5} [GA90], following equation has to be met.

$$\left(\frac{W}{L}\right)_3 = \left(\frac{W}{L}\right)_6 \cdot \frac{I_3}{I_6} \tag{2.22}$$

Since $I_{DS3} = I_{DS4} = {I_{DS5}}/{2}$, the above equation becomes,

$$\left(\frac{W}{L}\right)_3 = \frac{\left(W/L\right)_6}{2} \cdot \frac{I_7}{I_6} \tag{2.23}$$

Since M_4 and M_3 are matched, the size of M_4 is also obtained.

In the above discussion, we chose one specification to determine relevant parameters at each design step. However, other specifications must be checked at each design step. If some of the specifications haven't been met, adjustments must be made to insure all specifications have been met.

www.manaraa.com

CHAPTER 3. LOW-VOLTAGE OPERATIONAL AMPLIFIER DESIGN

In Chapter 2, some basic knowledge of the MOSFET and design procedures for two-stage operational amplifiers were introduced. In this chapter, design details of a 500mV low-voltage operational amplifier will be discussed. I will begin with reviewing previous work regarding low-voltage operational amplifiers design, followed by an introduction of the proposed structure for 500mV low-voltage operational amplifier.

3.1 Previous work

Many papers and books have been published on low-voltage operational amplifiers [EC96] [FM89] [HL85] [AB95]. With reduced power supply voltage, many operational amplifier architectures will lose operational range especially at their input stages. Thus operational amplifiers with large input signal swing are greatly desired. Such operational amplifiers often employed complementary differential pairs as an input stage as shown in Figure 3.1 [SI95], [HL85].

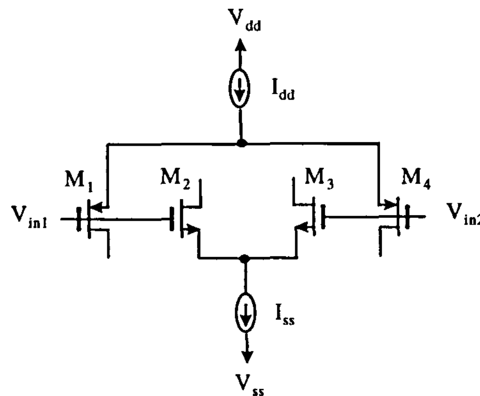

Figure 3.1 Complementary differential input stage

www.manaraa.com

By connecting an n-channel differential pair and a p-channel differential pair in parallel, the input stage can reach rail-to-rail. When the common mode voltage, $V_{CM,}$ is near the negative power supply voltage, only the p-channel pair is functional. When the common mode voltage, $V_{CM,}$ is near the positive power supply voltage, only the n-channel pair is functional. When V_{CM} is intermediate between the negative supply and positive supply, both the n-channel pair and p-channel pair will operate. An important design consideration associated with this kind of circuit is to keep the sum of transconductances of the complementary differential pairs $\left(g_m = g_{mn} + g_{mp}\right)$ constant in order to guarantee a constant gain-bandwidth product under different common-mode input voltages. The methods to keep g_m constant can be found in Satoshi Sakurai's work [SI95].

A threshold voltage tunable operational amplifier utilizing floating gate MOS transistors was also presented by Yu [YU93]. A floating gate MOS transistor cell is illustrated in Figure 3.2. Since a floating gate MOS transistor can have a very low threshold voltage without device scaling while still maintaining comparable characteristics to those of conventional MOS transistors, floating gate MOS transistors can be used as operational amplifier elements. However, the threshold tuning method employed a complicated implementation procedure. The floating gate transistor also

Figure 3.2 Floating gate MOS transistor cell

www.manaraa.com

does not compensate for temperature variation. Most importantly, the floating gate device requires specified processing steps that are normally not available in most of existing standard commercial semiconductor processes.

3.2 Threshold voltage tuning

Generally, the threshold voltage and the saturation voltage of MOS transistors for operation in the strong inversion region limits the minimum supply voltage. This limitation is given by the expression,

$$V_{\sup} \geq \max\left\{\left(V_{TN} + \left|V_{dsatp}\right|\right), \left(\left|V_{TP}\right| + V_{dsatn}\right)\right\} \tag{3.1}$$

For a current standard CMOS technology, this limitation will result in a minimum supply voltage of approximately 1.5V [MU96].

Conceptually, if we lower the threshold voltage to 0.2V, we can expect to obtain a 0.5V supply voltage. The floating gate MOS transistor discussed in the previous section is one approach. Another way to electrically lower the effective threshold voltage is to connect a DC voltage source in series with the gate as depicted in Figure 3.3. where,

$$\left|V'_T\right| = \left|V_T\right| - V_{DC} \tag{3.2}$$

By lowing the threshold voltage, we can apply a lower effective input voltage to obtain the same V_{GS} as shown in Figure 3.4. Since MOS transistors are implemented in standard process in both cases, they will have the same performance parameters such as g_m and g_o since they have the same V_{GS} and thus essentially the same I_D.

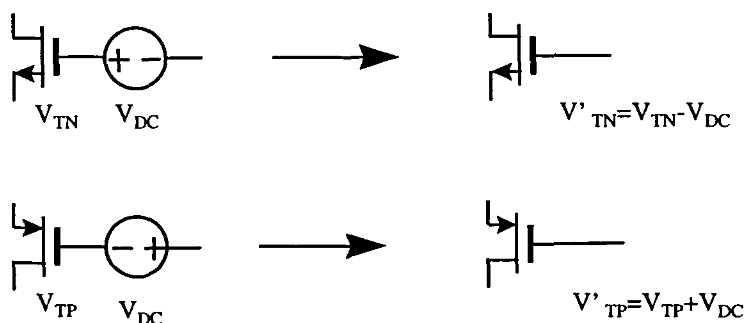

Figure 3.3 Threshold voltage tunable structure

www.manaraa.com

V_{in} $V_{in}' = V_{in} - V_{DC}$

$V'_{TN} = V_{TN} - V_{DC}$

Figure 3.4 Threshold voltage tuning effects

3.3 Threshold tunable low-voltage operational amplifier

As illustrated in the previous section, by connecting a DC voltage source in series with the gate of MOS transistors, we can electrically lower the effective threshold voltage. Using this method, we can connect a DC voltage to the gate of all the MOS transistors to design the operational amplifier. An example of an operational amplifier designed using this technique employing the two-stage architecture discussed in the previous chapter is shown in Figure 3.5. With the electrically reduced threshold voltages, the power supply voltage Vdd can be substantially reduced.

The two-stage operational amplifier is used to investigate the effects of threshold tuning to achieve effective power supply scaling. A feedback resistor Rz is inserted in series with the feedback capacitor C_C. It is well known that this resistor can be used to

Figure 3.5 Threshold tunable low-voltage operational amplifier

المنارة للاستشارات
www.manaraa.com

eliminate the effect of the right-half-plane zero resulting from feedforward through the compensation capacitor C_C. The resistor value is given by the expression

$$R \geq \left(\frac{C_C + C_I}{C_C}\right) \cdot \left(\frac{1}{g_m}\right) \tag{3.3}$$

where C_I is the load capacitor of the second stage and g_m is the transconductance of the second stage.

For the convenience of investigating the performance of the proposed low-voltage operational amplifier, comparisons between the original 3.3V standard two-stage operational amplifier and the proposed 500mV low-voltage operational amplifier are made. The same device sizes and tail currents are used in both the amplifiers.

Based on the equations (2.13)~(2.16)

Slew rate $$SR = \frac{I_5}{C_C}$$

First stage gain $$A_{v1} = \frac{g_{m2}}{g_{ds2} + g_{ds4}} = \frac{2g_{m2}}{I_5 \cdot (\lambda_2 + \lambda_4)}$$

Second stage gain $$A_{v2} = \frac{g_{m6}}{g_{ds6} + g_{ds7}} = \frac{g_{m6}}{I_6 \cdot (\lambda_6 + \lambda_7)}$$

Gain-bandwidth $$GB = \frac{g_{m2}}{C_C}$$

We can see that both of the operational amplifiers have the same key performance parameters.

3.4 500mV operational amplifier design

Depending on the discussion in the previous two sections, we can obtain the same key performance parameters in the low-voltage operational amplifier as in the standard 3.3V operational amplifier by maintaining the device sizes and tail currents while scaling down the effective threshold voltage. The DC voltage sources connected to the gate of all the MOS transistors will also differ slightly and this difference depends on whether the device is a pMOS transistor or an nMOS transistor. In the following simulation, I have scaled the threshold voltage down to 15 percent of the standard value.

المنارة للاستشارات
www.manaraa.com

The device sizes used in the simulation are given in Table 2.1. These sizes were determined by following the procedure given in Chapter 2.

Level 13 0.5μ CMOS models were used in the simulation. Although the minimum size used in the design is 2μ, due to available MOSIS HP technologies and fabrication schedule, the circuit was supposed to fabricated in 0.5μ CMOS process. However, level 3 0.5μ CMOS models were also used in simulation for comparison purpose.

Table 3.1 Device sizes used in the two-stage operational amplifier

	M1	M2	M3	M4	M5	M6	M7	M8	I_5	Rz	Cc
W(μ)	20	20	80	80	20	398	48	20	20 μA	12K	2P
L(μ)	2	2	2	2	2	2	2	2			

Figure 3.6 shows the frequency response of the original 3.3V two-stage operational amplifier operating at T=25^{0}C, (a) shows the magnitude response while (b) shows phase response. In order to have 20uA tail current, the biasing resistor R is equal to

$$R \approx \frac{V_{DD} - V_T}{I_8} \approx \frac{3.3 - 0.8}{20} \approx 125K \tag{3.4}$$

Figure 3.7 shows the preliminary frequency response of the proposed 500mV low-voltage operational amplifier also operating at T=25^{0}C. (a) shows the magnitude response and (b) shows phase response. In order to provide the same tail current, the biasing resistor R in the 500mV design is

$$R \approx \frac{V_{DD} - V_T}{I_8} \approx \frac{0.5 - 0.15}{20} \approx 17K \tag{3.5}$$

From comparisons between Figure 3.6 and Figure 3.7, we can see that the proposed 500mV low-voltage amplifier has comparable magnitude and phase performance to that of the original 3.3V structure. The original 3.3V operational amplifier demonstrates 75dB DC gain, 10MHz unity gain bandwidth and a 60° phase margin. The proposed 500mV low-voltage operational amplifier achieves 70dB DC gain, 8MHz unity gain bandwidth and a 62° phase margin.

المنارة للاستشارات

www.manaraa.com

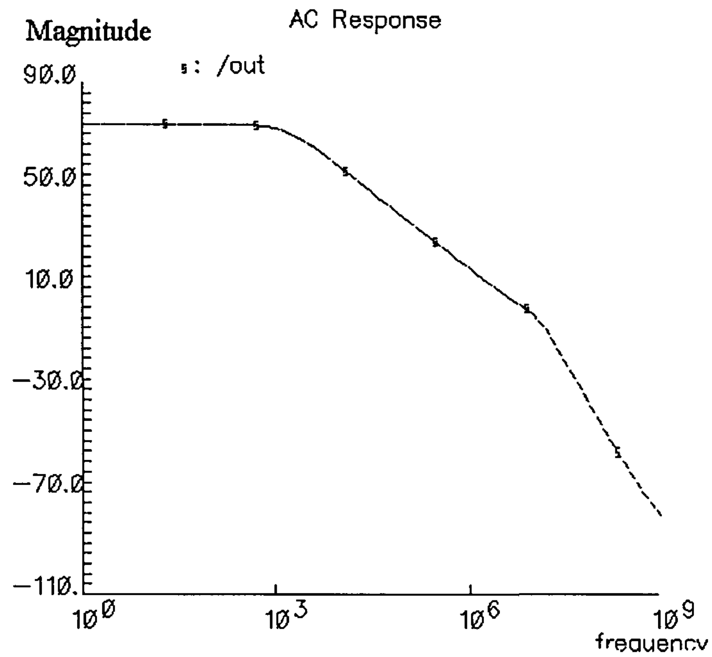

(a)

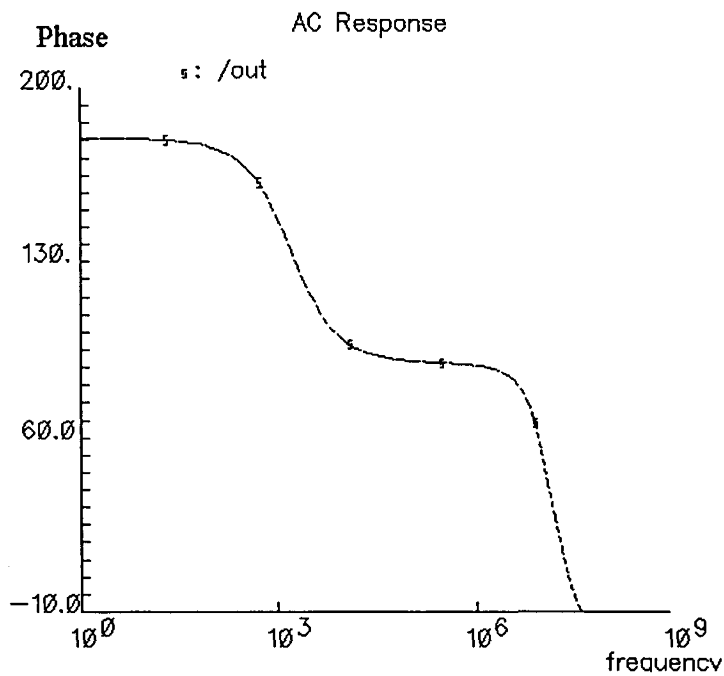

(b)

Figure 3.6 Frequency response of the original two-stage operational amplifier

(a) Magnitude response (b) Phase response

المنارة للاستشارات
www.manaraa.com

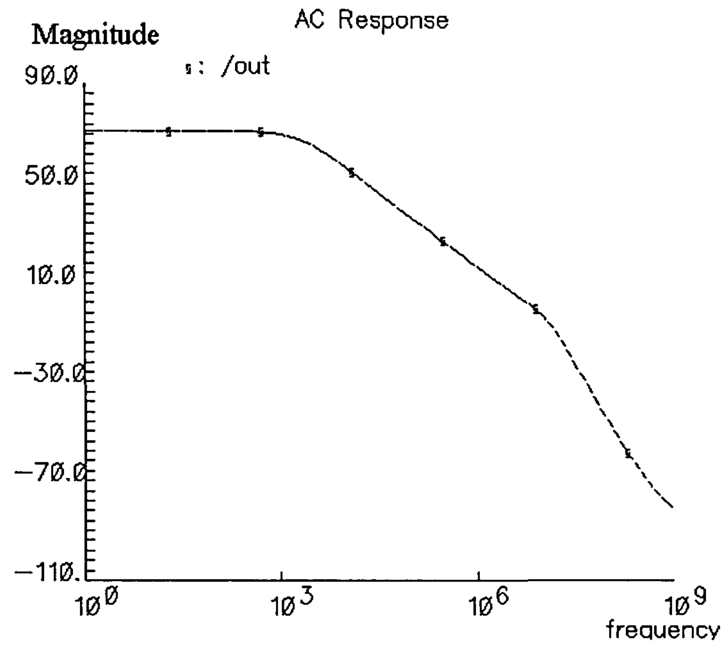

(a)

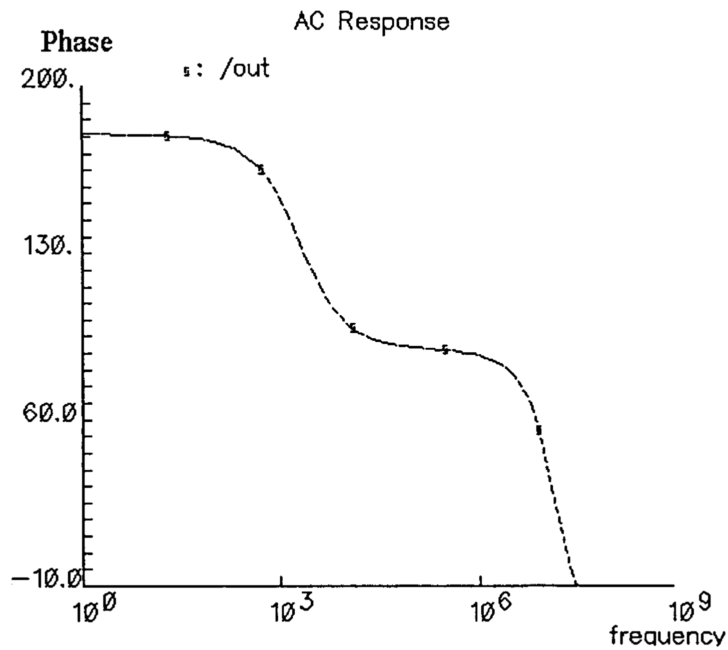

(b)

Figure 3.7 Frequency response of the proposed 500mV low-voltage operational amplifier

(a) Magnitude response (b) Phase response

www.manaraa.com

3.5 DC voltage source

Ideal DC voltage sources were connected to the gate of MOS transistors in the preliminary simulation. However, these DC voltage sources are implemented with capacitors charged periodically to keep the voltage on the capacitors constant. Figure 3.8 shows the basic approach for this implementation.

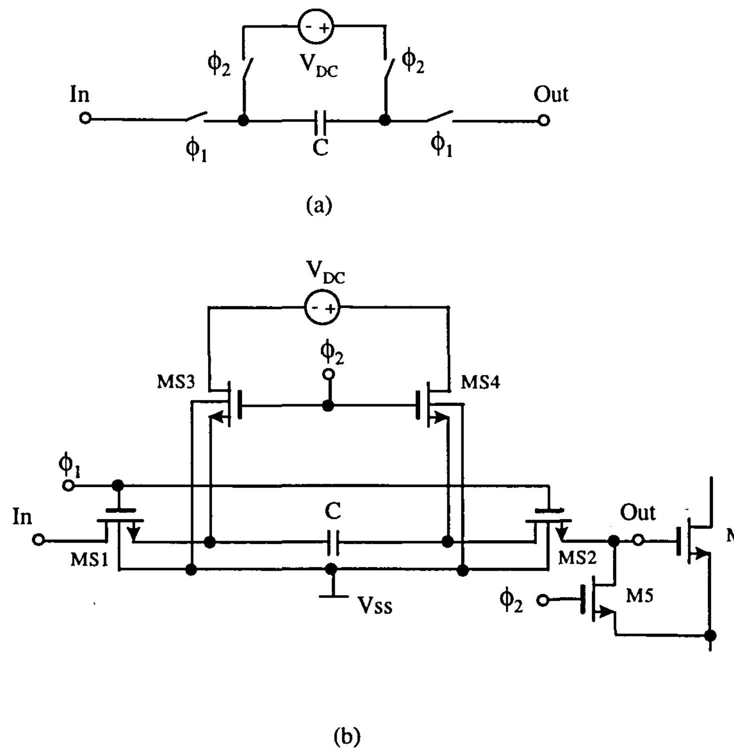

Figure 3.8 DC voltage source (a) Symbol (b) Circuit implementation

Figure 3.8 (a) shows the DC voltage representation. Figure 3.8 (b) shows a circuit implementation. Signals ϕ_1 and ϕ_2 are two phase nonoverlapping clocks. During ϕ_2, the reference voltage will charge the capacitor C to V_{DC}. During ϕ_1, the capacitor charged to V_{DC} will be connected to the gate of MOSFET M in the operational amplifier circuit and works as the DC voltage source in Figure 3.5. Since the input resistance of MOS transistors is very large, the charge on the capacitor C can be maintained for a log time. The nonideal effects of limited time storage of charge on C must nonetheless be investigated. To investigate these effects, consider the capacitor in series with the gate of

المنارة للاستشارات
www.manaraa.com

M6 of Figure 3.5. Figure 3.9 shows this capacitor along with the small-signal loading impressed by the preceeding and following stages. In Figure 3.9, the components are defined by

$$R_1^{-1} = R_{ds2}^{-1} + R_{ds4}^{-1} \quad (3.6)$$

$$C_1 = C_{gd2} + C_{gd4} + C_{db2} + C_{db4} \quad (3.7)$$

$$R_2 = R_{in6} \quad (3.8)$$

$$C_2 = C_{gs6} \quad (3.9)$$

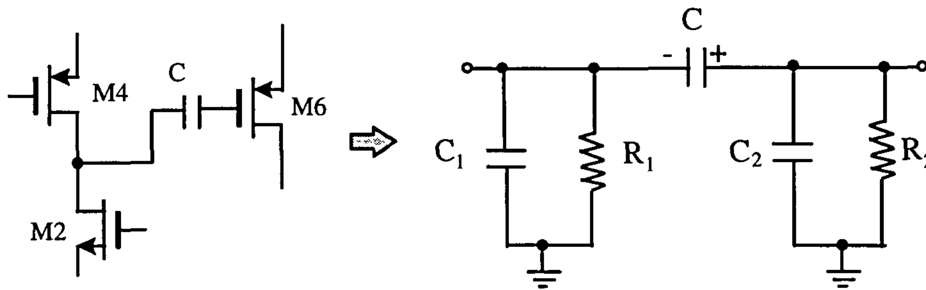

Figure 3.9 DC effects in the switched capacitor circuits

R_{in6} is the input impedance of the MOS transistor M6, which is of the order of 10^{10} and is much larger than R_1. Assuming capacitor C is much larger than C_1 and C_2, the time constant of the above circuit is about

$$\tau \approx R_{in} \cdot C \approx 5\times10^{10} \times 5\times10^{-12} = 0.25S \quad (3.1)$$

That means charge on the capacitor can be kept for a long time so that the frequency of ϕ_1 and ϕ_2 can be very low. On the other hand capacitor C charging is very fast, so that ϕ_2 can be a pulse. The typical signal waveforms for ϕ_1 and ϕ_2 are shown in Figure 3.10.

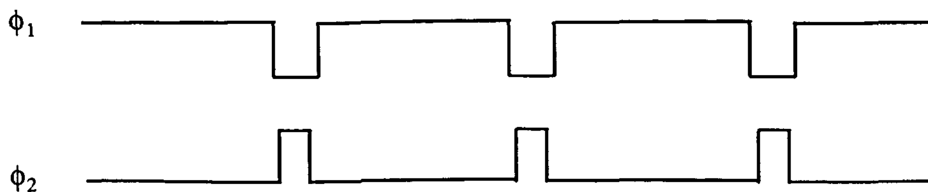

Figure 3.10 Waveform for ϕ_1 and ϕ_2

www.manaraa.com

The small signal model for the capacitor-MOSFET combination is shown in Figure 3.11. In this figure, C is the switched capacitor, C_1 is the gate capacitor, C_2 is the load capacitor. The switched capacitor C has two effects. It presents a capacitive load to the previous stage, which will affect the pole locations of the operational amplifier. As part of a voltage divider with C_1, it will affect the DC gain. If we assume C is much larger than C_1, then the load capacitor of the previous stage C_{load} and voltage v_1 on C_1 are equal to,

$$C_{load} = \frac{C \cdot C_1}{C + C_1} \approx C_1 \tag{3.11}$$

$$v_1 = \frac{C}{C + C_1} \cdot v_{in} \approx v_{in} \tag{3.12}$$

These two equations indicate that the load effect and the voltage divider effect are negligible if the switched capacitor C is much larger than the gate capacitor of the input MOS transistor. Hence connecting a capacitor in series with the gate of the transistor will not affect the frequency dependent performance of operational amplifiers.

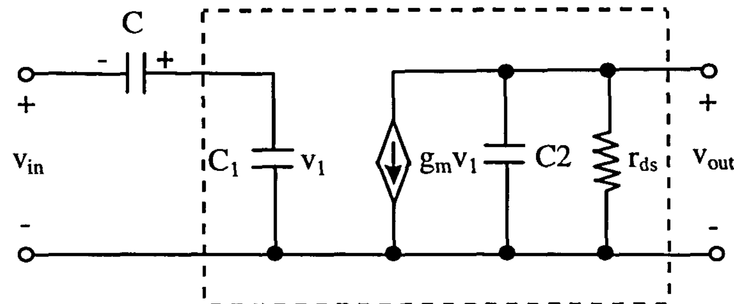

Figure 3.11 Small-signal model considering the capacitor effects

The effects of the practical implementation of the switched capacitor will mow be considered. Note that there is an nMOS transistor MS5 connected to the gate of the input transistor in Figure 3.8. This transistor is used to discharge charge accumulated on the gate of the input transistor due to substrate leakage current of the switched transistors due to the reverse biased diffusion-substrate junctions modeled by the diode in Figure 3.12.

www.manaraa.com

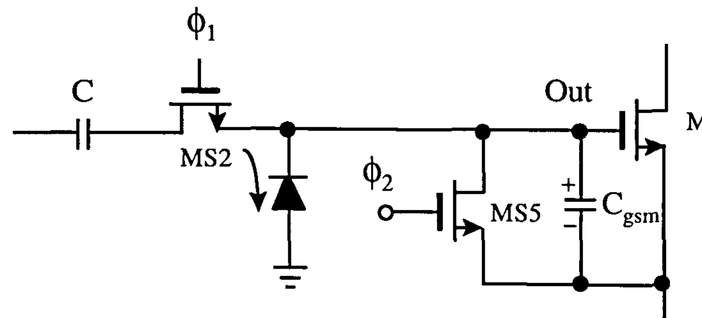

Figure 3.12 Leakage current effects and discharge circuit

The current flowing through the reverse biased diode will constantly charge the gate capacitor of the input transistor M. The charge accumulated on the gate capacitor has no path to be discharged so an additional discharge path is added to discharge any accumulated charge. The transistor M3 in Figure 3.12 provides such a path during ϕ_2.

In Figure 3.8, it is also worth noting that substrate is connected to a negative supply voltage V_{SS}. This is because the switch transistors in the voltage cells for pMOS transistors must transfer negative voltage, in order to guarantee the source and bulk pn junction is reverse biased, the substrate has to be connected to negative voltage.

Up till now, we have discussed the 500mV operational amplifier architecture. It has been shown that the proposed structure can have performance parameters comparable to those of the standard 3.3V operational amplifier.

3.6 Simulation results

In the previous section, a switched capacitor that serves as a voltage source was investigated. However, the switched capacitor circuit will not have a DC path in Hspice AC analysis. The switched capacitor is simulated separately for the transient response. A test circuit is used in the AC analysis which takes care of all the parasitic effects of the switched capacitor circuit meanwhile it can establish a DC path. Figure 3.13 shows the circuit used in the simulation. Two transistors with the gate connected to V_{DD} represent MS1 and MS2 when they are connected into the circuit in Figure3.8. V_{DC} represents the

www.manaraa.com

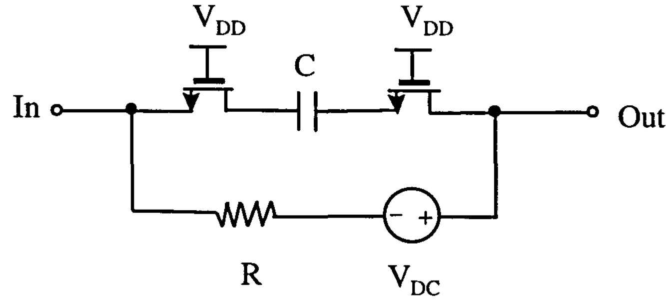

Figure 3.13 Simulation circuit for the switched capacitor

DC voltage on capacitor C. A very large resistor is connected in series with the DC voltage, so that the voltage source plays no role other than providing the proper quiescent voltage.

Figure 3.14 shows the frequency response of the 500mV low-voltage operational amplifier. Simulation results give a DC gain of 68dB, 7.8MHz unitygain bandwidth and a 65° phase margin. The reason of the 2dB decrease in the DC gain from what was obtained in the simulation results of Figure 3.14 is due, in part, to the voltage divider effect of the switched capacitor with the gate-source capacitance as was discussed in the previous section. With reduced DC gain, the second pole increased in magnitude thus improving the phase margin as shown in the simulation results.

More detailed simulation results are provided in Table 3.2 which shows the low frequency gain A_{DC}, the unity gain bandwidth frequency f_u and the phase margin ϕ_M for different V_{CM}. According to the table, the operational amplifier has about a 250mV common mode input range. The positive common mode voltage range is determined by expression [AH87].

$$V_{in(\max)} = V_{DD} + V_{T1eq} - |V_{T3eq}| - \left(\frac{I_5}{\beta_3}\right)^{1/2} \tag{3.13}$$

This expression gives a maximum positive common voltage of 450mV because the second term and the third term are almost equal and the fourth term is about 50mV.

The negative common voltage range is determined by expression

المنارة للاستشارات
www.manaraa.com

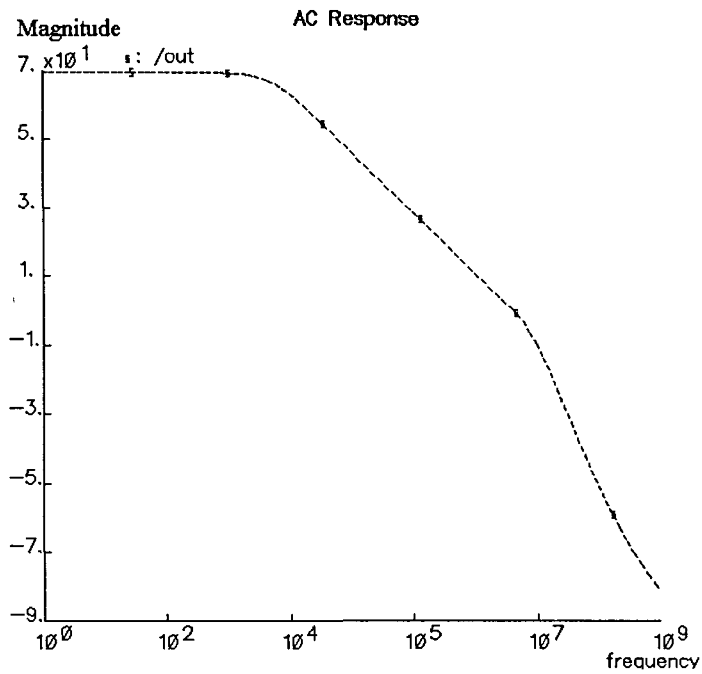

(a)

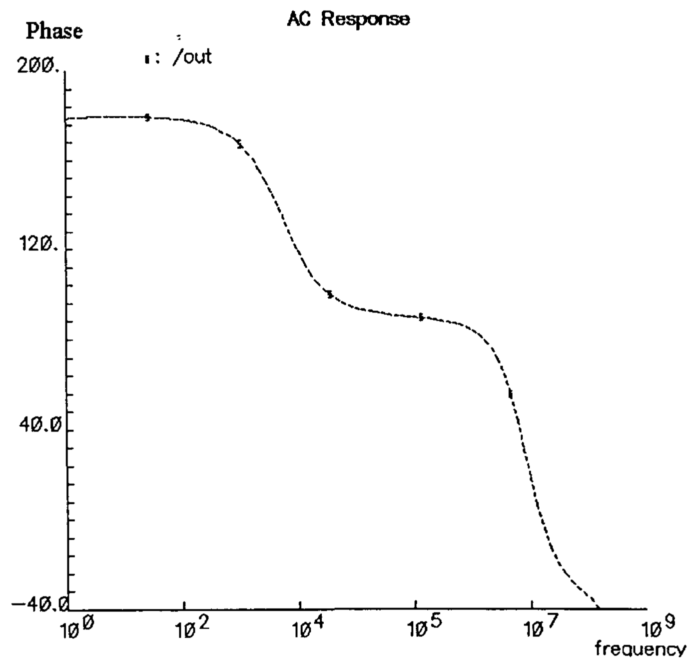

(b)

Figure 3.14 Frequency response of the 500mV low-voltage operational amplifier

(a) Magnitude response (b) Phase response

المنارة للاستشارات

www.manaraa.com

Table 3.2 Simulated frequency response of the 500mV low-voltage operational amplifier

V_{CM} (mV)	A_{DC} (dB)	f_u (MHz)	PM (^{O})
460	51	5.7	69
440	52	6.0	67
420	60	6.2	67
400	65	7.0	66
380	67	7.4	65
360	68	7.8	65
340	68	7.8	65
320	68	7.8	65
300	68	7.8	65
280	67	7.2	66
260	65	7.0	67
240	62	6.4	68
220	57	6.1	69
200	52	5.9	70

$$V_{in(\min)} = V_{T1eq} + V_{sat5} + \left(\frac{I_5}{\beta_1}\right)^{1/2} \tag{3.14}$$

In the above equation, the saturation voltage is about 50mV as in the standard 3.3V operation amplifier. V_{T1eq} is about 120mV. The last term $\left(\frac{I_5}{\beta_1}\right)^{1/2}$ is about 50mV, hence the minimum common voltage is about 220mV.

Two close loop characteristics, the unity gain DC transfer characteristic and the step response were simulated. Results are shown in Figure 3.15.

المنارة للاستشارات

www.manaraa.com

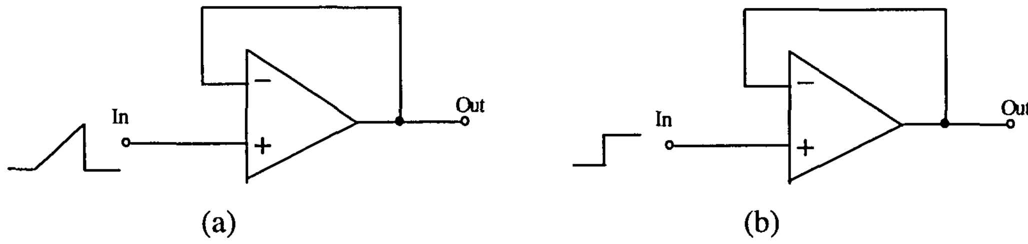

Figure 3.15 (a) Test circuit for unity gain DC transfer characteristics
(b) Test circuit for unity gain step response

Figure 3.16 (a) shows the unity gain DC transfer characteristic of the 3.3V operational amplifier. Figure 3.16 (b) shows the unity gain DC transfer characteristic of the 500mV low-voltage operational amplifier. The 3.3V operational amplifier has very good linear DC transfer characteristic within the range from 500mV to 3.4V. The 500mV low-voltage operational amplifier has very good linear DC transfer characteristic within the range from 50mV to 480mV.

Figure 3.17 (a) shows the unity gain step response for a 100mV input step for the 3.3V operational amplifier. Figure 3.17 (b) shows the unity gain step response of the 500mV low-voltage operational amplifier. In this simulation, the step was also 100mV. Simulation results indicate that the settling time of 3.3V operational amplifier is about 50nS. The settling time of the 500mV low-voltage operational amplifier is also about 50nS. These results are expected since the tail current and compensation capacitor are the same for both the 3.3V operational amplifier and the 500mV low-voltage operational amplifiers.

$$\Delta t = \frac{\Delta v}{SR} = \frac{\Delta v}{I_5/C_c} = \frac{\Delta v \cdot C_c}{I_5} \tag{3.15}$$

We can note in Figure 3.16 that there is ripple on the step response of the 3.3V operational amplifier while there is no ripple on the step response of 500mV low-voltage operational amplifier. This can be explained because the 500mV low-voltage operational

المنارة للاستشارات
www.manaraa.com

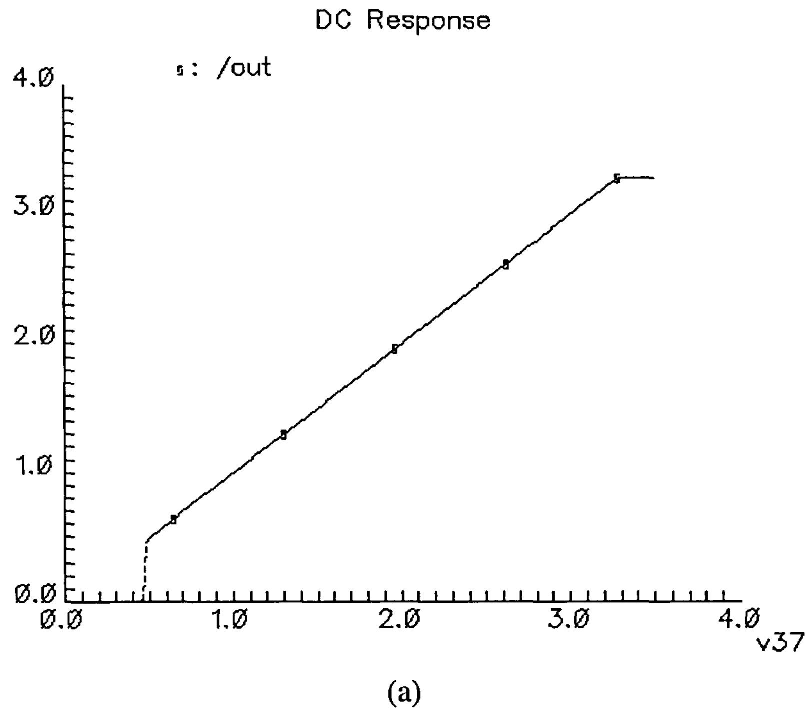

(a)

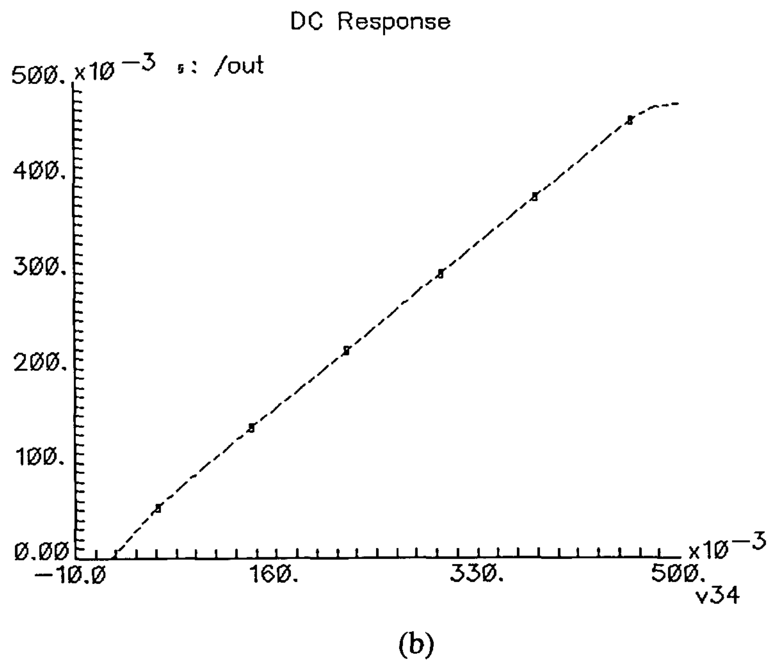

(b)

Figure 3.16 (a) Unity gain DC transfer characteristics of the 3.3V operational amplifier

(b)Unity gain DC transfer characteristics of the 500mV operational amplifier

www.manaraa.com

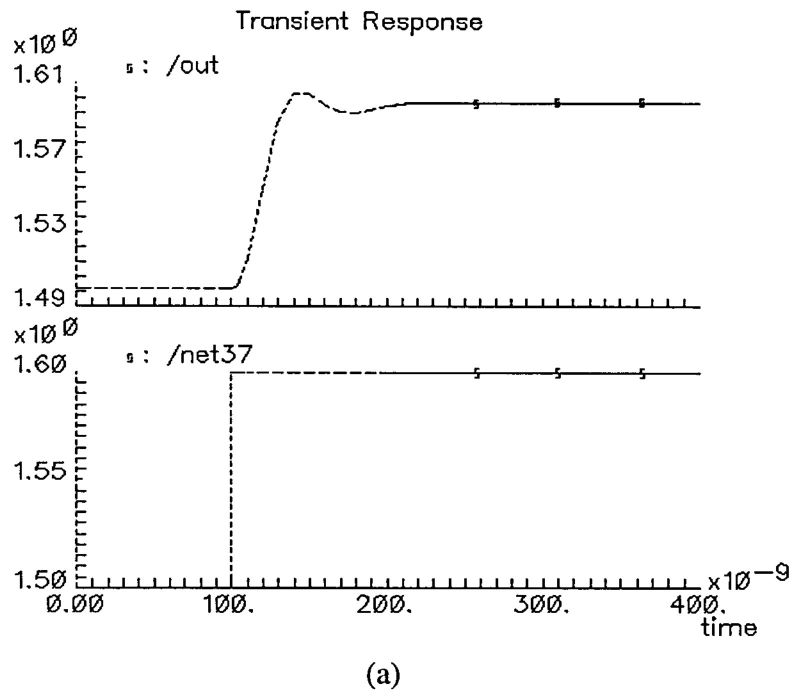

(a)

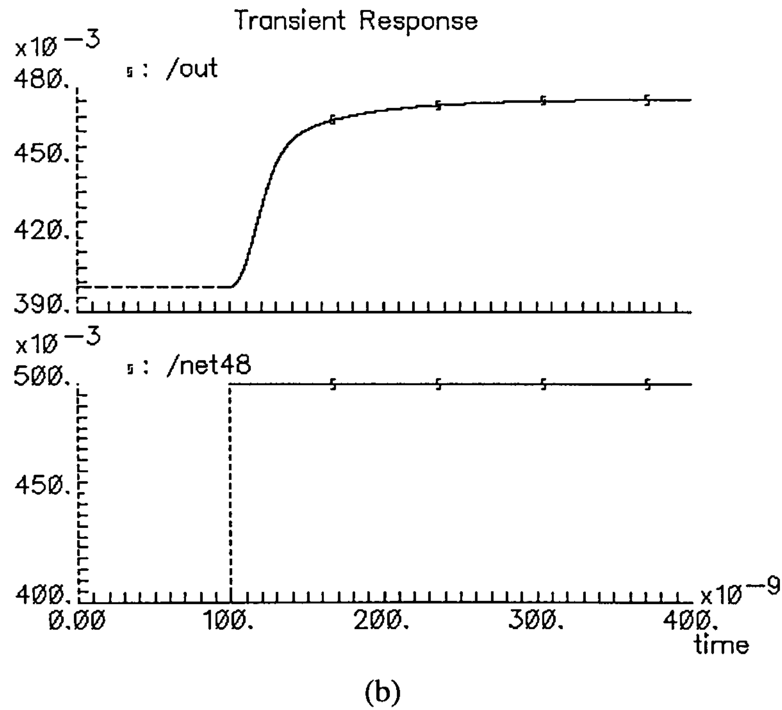

(b)

Figure 3.17 (a) Unity gain impulse response of the 3.3V operational amplifier
(b) Unity gain impulse response of the 500mV operational amplifier

www.manaraa.com

amplifier has a larger phase margin than the 3.3V operational amplifier. A modest reduction in the compensation capacitor for the 500mV operational amplifier should provide some improvement in the settling time.

3.7 Conclusions

A 500mV low-voltage operational amplifier design was investigated in this chapter. A circuit implementation was presented and parasitic effects are considered. Simulations results indicated that the 500mV low-voltage amplifier has comparable key performance parameters to a 3.3V operational amplifier as can be seen from the summarizes in Table 3.3.

Table 3.3 Comparisons of performance parameters of the two operational amplifiers

	Standard amplifier	Proposed amplifier
Supply voltage	3.3V	0.5V
DC-gain	75dB	68dB
GBW	10MHz	7.8MHz
PM	60°	65°
Tail current	20µA	20µA
Power dissipation	200µW	35µW

As anticipated, simulation results also indicated that these two operational amplifiers have similar unity gain close loop performance. Although the 500mV low-voltage operational amplifier has a much smaller common mode input range, it is still reasonable for such a low supply voltage.

Figure 3.18 shows the layout of the 500mV low-voltage operational amplifier core and the switched capacitor voltage sources. This layout was done in a 0.5µ CMOS process.

المنارة للاستشارات

www.manaraa.com

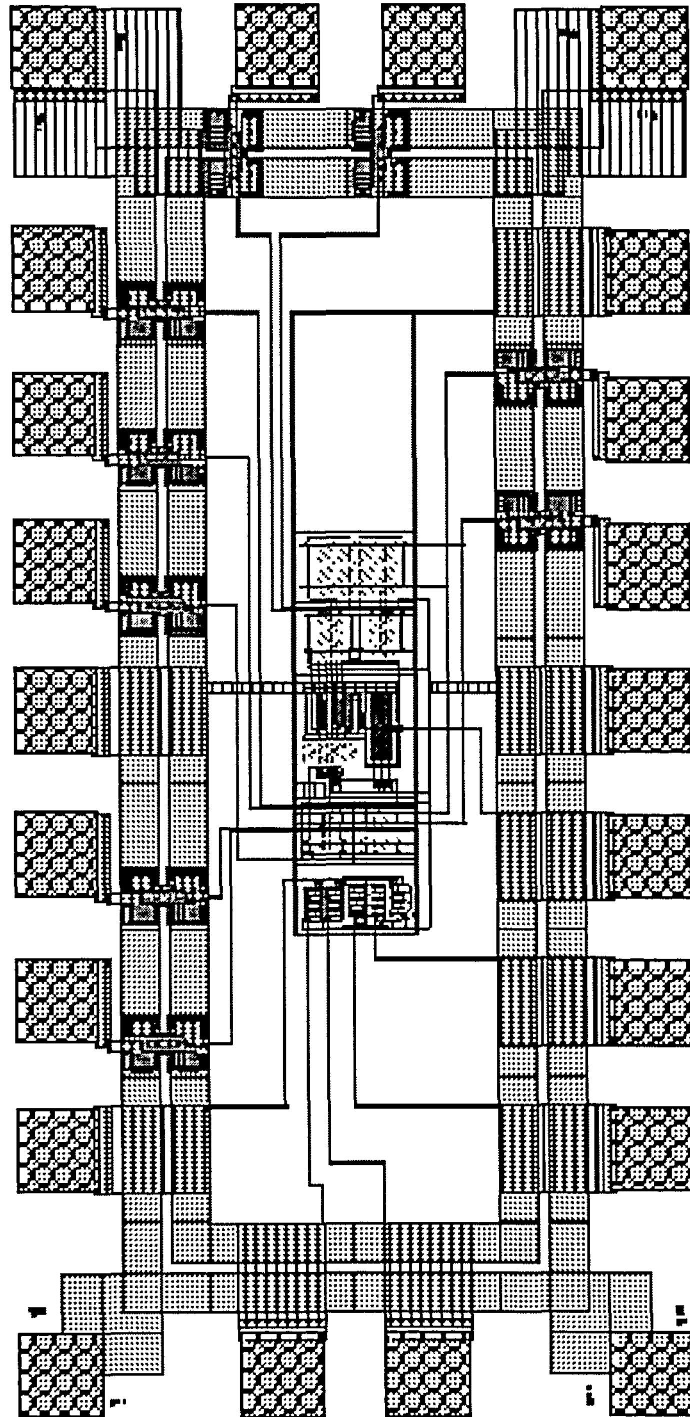

Figure 3.18 Layout of the 500mV low-voltage operational amplifier

www.manaraa.com

CHAPTER 4. SUPPLEMENTARY CIRCUIT IMPLEMENTATIONS

In Chapter 3, we discussed the design of the 500mV low-voltage operational amplifier. Methods for generating the negative voltage V_{SS}, for determining the voltage V_{DC} that is stored on the series capacitor C and generation of the clocks ϕ_1 and ϕ_2 were not considered. In this chapter, the supplementary circuits need to realize these functions for the low-voltage operational amplifier will be given.

4.1 Supplementary circuits

As mentioned in Chapter 1, low-voltage system may need some supplementary circuits to provide an appropriate operation environment. The 500mV ultra low-voltage operational amplifier system architecture contains three main blocks, the operational amplifier core, the reference voltage generator and the oscillator. The block diagram of such a system is shown in Figure 4.1. In Chapter 3, the operational amplifier core was discussed, the reference voltage and oscillator will be explored in this chapter.

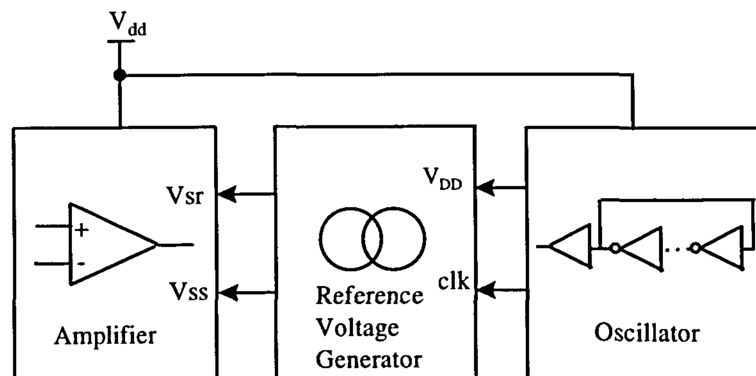

Figure 4.1 Low-voltage operational amplifier architecture

www.manaraa.com

The reference voltage generator provides the DC voltage source and the negative supply voltage for the operational amplifier. The oscillator provides clocks for the switched capacitors and the charge pump which pumps the 500mV supply voltage up to 3.3V. The 3.3V supply is needed to extract the reference DC voltage. Throughout the text, V_{DD} refers to 3.3V supply voltage and V_{dd} refers to 500mV supply voltage.

4.2 Reference voltage generation

In a standard process, threshold voltage will inherently have a 100mV to 200mV variation due to process and temperature variations. If a constant DC voltage source is used as the reference voltage source in Figure 3.5, the equivalent nominal threshold voltage will be scaled down by the same amount but the variation will be the same as for the original transistor. This variation is intolerable for very low-voltage applications [ST95]. This effect is shown in Figure 4.2 (a).

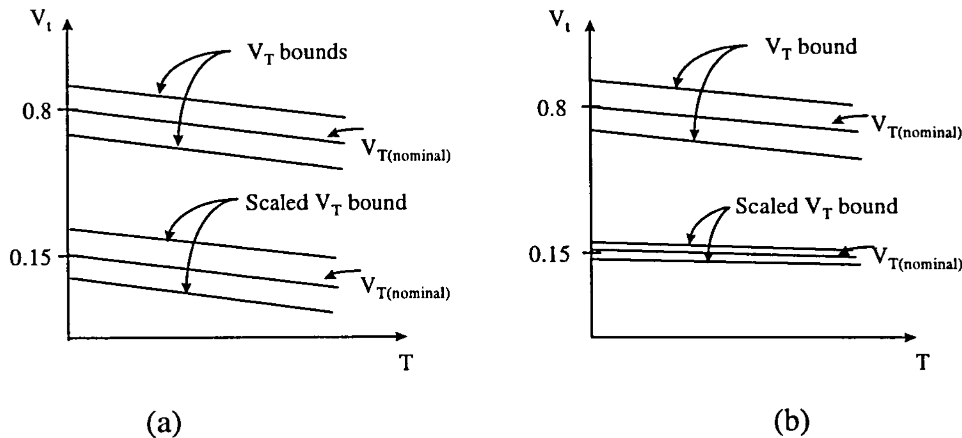

Figure 4.2 Threshold voltage variation effects

(a) Threshold voltage scaling (b) Threshold voltage scaling with compensation

However, if the voltage source can follow the threshold variation, then it can compensate for the threshold voltage variation and hence the equivalent threshold voltage will have a relatively constant value as desired. That is to say, $V_{Teq} = \theta \cdot V_T$ is preferred over $V_{Teq} = V_T - V_{const}$. Alternatively, we can also generate an equivalent threshold

www.manaraa.com

voltage that is independent of V_T. The desired threshold scaling is shown in Figure 4.2 (b). Both approaches will be considered.

One way to realize such voltage source is to first extract the threshold voltage itself and then attenuate or level shift this voltage to obtain V_{DC}.

One circuit that can be used to extract the threshold voltages is shown in Fig. 4.3.

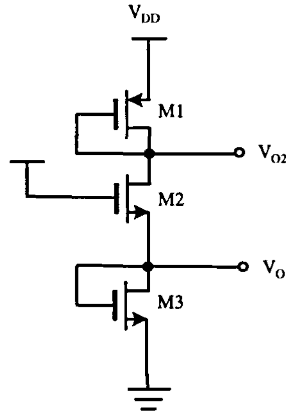

Figure 4.3 Threshold voltage extraction

According to equation (4.1),

$$I = K_3 \cdot (V_{GS3} - V_{T3})^2 = K_2 \cdot (V_{GS2} - V_{T2})^2 = K_1 \cdot (V_{GS1} - V_{T1})^2 \quad (4.1)$$

where $K = \frac{\mu \cdot C_{ox} \cdot W}{L}$

If $\left(\frac{W}{L}\right)_1$ and $\left(\frac{W}{L}\right)_3$ are large and $\left(\frac{W}{L}\right)_2$ is small, it follows that V_{GS1} is very close to V_{TP} and V_{GS3} is very close to V_{TN}. It remains to scale and/or shift the voltages V_{GS1} and V_{GS3}.

The two approaches to generate V_{Teq} are denoted by Approach 1 and Approach 2:

Approach 1: $V_{Teq} = \alpha \cdot V_T$

$$V_{DC} = -(1-\alpha) \cdot V_T \quad (4.2)$$

Approach 2: $V_{Teq} = V_{const}$

$$V_{DC} = -V_T + V_{const} \quad (4.3)$$

للاستشارات المنارة
www.manaraa.com

In Approach 1, the equivalent threshold voltage is a portion of the original threshold voltage, so that the threshold voltage maintains the same relative variation as the original one. In Approach 2, the threshold voltage variation is eliminated and the equivalent threshold voltage is a constant voltage. Both approaches will be discussed here. The attenuator will be implemented by an active linear voltage attenuator as shown in Figure 4.4 [KI95].

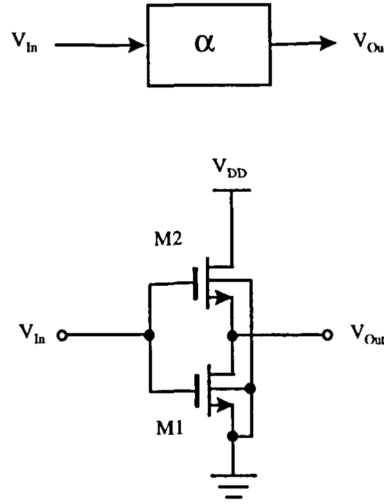

Figure 4.4 Block diagram and circuit of an Attenuator consisting of two nMOSFETs

The circuit operates as a linear voltage attenuator when M1 is in the ohmic region and M2 is in the saturation region. Assuming the zero bias threshold voltage of both nMOSFETs is V_{TN}, the operating condition will be met if

$$V_{T1} < V_{In} < V_{DD} + V_{T2} \tag{4.4}$$

where

$$V_{T1} = V_{TN} \text{ and } V_{T2} = V_{TN} + \gamma \cdot \left(\sqrt{\phi + V_{Out}} - \sqrt{\phi}\right) \tag{4.5}$$

The drain currents of M1 and M2 are

$$I_{D1} = K' \cdot \frac{W_1}{L_1} \cdot \left(V_{In} - V_{T1} - \frac{V_{Out}}{2}\right) \cdot V_{Out} \tag{4.6}$$

$$I_{D2} = K' \cdot \frac{W_2}{2L_2} \cdot \left(V_{In} - V_{T2} - V_{Out}\right)^2 \tag{4.7}$$

المنارة للاستشارات
www.manaraa.com

Equating the two currents in (4.6) and (4.7), we obtain

$$2 \cdot \theta \cdot \left(V_{In} - V_{T1} - \frac{V_{Out}}{2} \right) \cdot V_{Out} = \left(V_{In} - V_{T2} - V_{Out} \right)^2 \tag{4.8}$$

where

$$\theta = \frac{W_1 / L_1}{W_2 / L_2} \tag{4.9}$$

If the body effect is negligible so that V_{T1} and V_{T2} are equal to V_{TN}. The DC transfer characteristic relating V_{In} and V_{Out} becomes a linear equation,

$$V_{Out} = \alpha \cdot \left(V_{In} - V_{TN} \right) \tag{4.10}$$

where α is the small signal attenuation factor of the attenuator. In this case, the relationship between θ and α is given by the expression

$$\alpha = 1 - \sqrt{\frac{\theta}{\theta + 1}} = 1 - \sqrt{\frac{W_1 / L_1}{W_1 / L_1 + W_2 / L_2}} \tag{4.11}$$

When the body effect can't be neglected, the relationship between the input and the output is still nearly linear [KI95]. The simulation result of this attenuator is shown in Figure 4.5 where the body effect is considered.

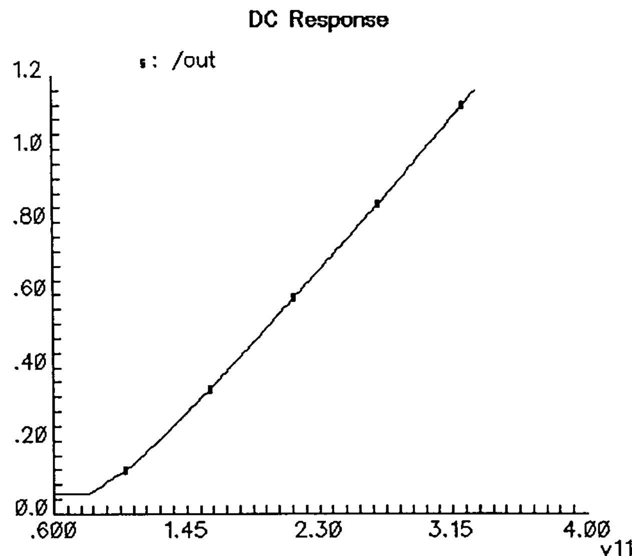

Figure 4.5 DC transfer characteristic of the attenuator consisting of two nMOSFETs

المنارة للاستشارات

www.manaraa.com

The result indicates that the attenuator consisting of two nMOS transistors has very good linearity within the input range from 1.2V to 3.3V. The attenuator can not be used to attenuate voltage V_{TN} because $V_{TN} < 1.2V$. To solve this problem, two types of attenuators will be used for reasons that become apparent later. Thus consider the attenuator consisting of two pMOSFETs as shown in Figure 4.6.

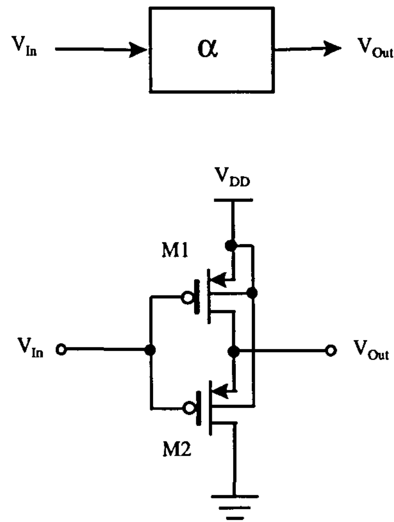

Figure 4.6 Block diagram and circuit of an attenuator consisting of two pMOSFETs

Similar to the analysis of the attenuator consisting of two nMOSFETs, the DC transfer characteristic of this attenuator is,

$$V_{Out} = \alpha \cdot V_{In} - \alpha \cdot V_{TP} + (1-\alpha) \cdot V_{DD} \qquad (4.12)$$

where

$$\alpha = 1 - \sqrt{\frac{W_1/L_1}{W_1/L_1 + W_2/L_2}} \qquad (4.13)$$

The simulation result of this attenuator is shown in Figure 4.7. This attenuator has very good linear DC transfer characteristic within the range from 0 to 2V.

www.manaraa.com

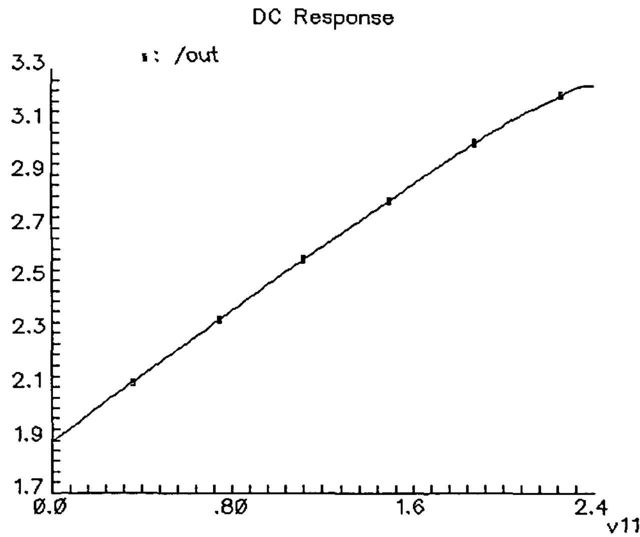

Figure 4.7 DC transfer characteristic of the attenuator consisting of two pMOSFETs

Consider now the circuit of Figure 4.8, where the two Attenuator I's are n-channel attenuators and the two Attenuator II's are p-channel attenuators. It follows from (4.10) and (4.12) that

$$V_2 = \alpha_P \cdot V_1 - \alpha_P \cdot V_{TP} + (1-\alpha_P)\cdot V_{DD} \tag{4.14}$$

$$V_4 = \alpha_P \cdot V_3 - \alpha_P \cdot V_{TP} + (1-\alpha_P)\cdot V_{DD} \tag{4.15}$$

$$V_6 = \alpha_N \cdot (V_5 - V_{TN}) \tag{4.16}$$

$$V_8 = \alpha_N \cdot (V_7 - V_{TN}) \tag{4.17}$$

where α_N and α_P are the attenuator gains of Attenuator I and Attenuator II respectively.

From the observation following (4.1), we have

$$V_3 \approx V_{Tn} \tag{4.18}$$

$$V_5 \approx V_{DD} + V_{TP} \tag{4.19}$$

Finally, since $V_1 = 0$ and $V_7 = V_{DD}$, it follows from (4.14)-(4.19) that

$$V_4 - V_2 = \alpha_P \cdot V_{TN} \tag{4.20}$$

$$V_6 - V_8 = \alpha_N \cdot V_{TP} \tag{4.21}$$

These are depicted on Figure 4.8.

www.manaraa.com

Figure 4.8 DC reference voltage generator for Approach 1

Note that since $\alpha_N . V_{TP}$ and $\alpha_P . V_{TN}$ become the equivalent threshold voltages for the p-channel and n-channel transistors, both the total and precise control of the thresholds is possible. In applications that would benefit from multiple threshold voltages, multiple DC reference generators with varying gains can be generated. Finally, since the threshold voltage due to process variations will be the same for all transistors on a die, the effective threshold voltage for all device using the reference of Figure 4.8 will be inherently compensated for process varations.

As we can see, in order to extract the threshold voltage and make the attenuators work, supply voltages higher than 500mV has to be used for the extraction circuits and attenuation circuits. A charge pump will be used to pump 500mV supply voltage up to 3.3V and will be discussed in the next section.

A circuit suitable for generation of V_{DC} for Application II appears in Figure 4.9. The two reference generators are used to generate a voltage reference. REFN generates the reference voltage relative to ground and REFP generates the reference voltage relative to V_{DD}. The resistors R1-R4 depict scaling of the reference voltages and would be implemented with active devices. Alternatively, the reference generators an reference scaling circuits could be replace with a simple 3-transistor voltage generator connected between V_{DD} and ground if extreme precision in the threshold voltages is not

المنارة للاستشارات
www.manaraa.com

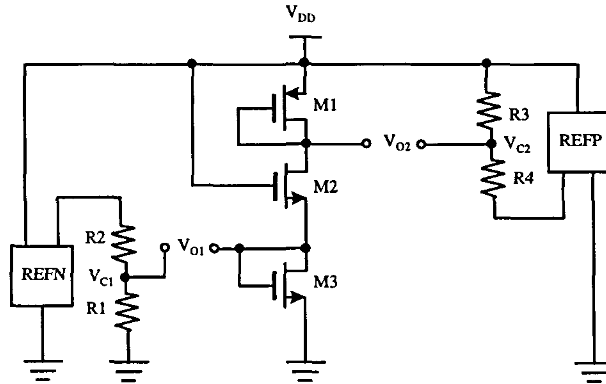

Figure 4.9 DC reference voltage generator for Approach 2

needed. It follows that

$$V_{O1} = V_{C1} - V_{TN} \tag{4.22}$$

and

$$V_{O2} = V_{C1} - V_{TP} \tag{4.23}$$

These are the DC reference voltages needed for Approach 2.

4.3 High voltage and negative voltage generator

The high supply voltage for the threshold voltage extraction circuits and attenuator circuits is developed from the 500mV supply voltage with an on-chip charge pump. One implementation of a high voltage generator is shown in Figure 4.10. The high voltage generator consists of an oscillator, a charge pumping circuit and a voltage regulator.

The oscillator generates $\phi 1$ and $\phi 2$, two phases nonoverlapping clocks. Nonoverlapping clocks are needed to guarantee there will be no leakage between switchs so that the pumping efficiency will be high. The charge pump works as follows: when $\phi 1$ and $\phi 2$ are both high and the pMOSFETs will be turned off and the power supply V_{DD} will charge the capacitors through the nMOSFETs. When $\phi 1$ and $\phi 2$ are both low, the nMOSFETs will be turned off, the capacitors will be connected in series and all the voltage on the capacitors will be summed and transferred to the output. The clock is chosen to be between 100KHz to 1MHz. If the clock frequency is too low, less charge will be transferred to the output during unit time period. If the clock frequency is too high

المنارة للاستشارات
www.manaraa.com

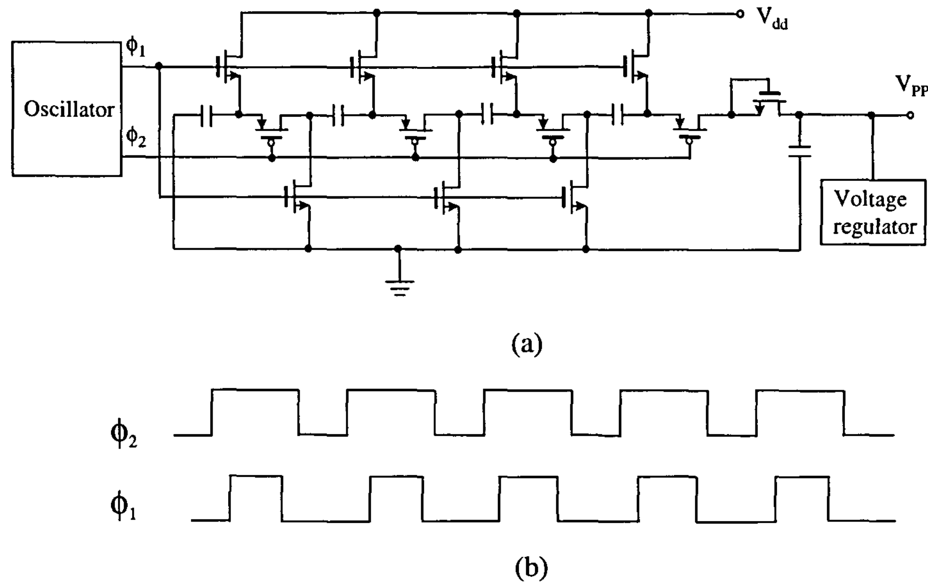

(a)

φ2

φ1

(b)

Figure 4.10 (a) Charge pump circuit
(b) Clock waveforms

the switching between the nMOSFETs and the pMOSFETs will be too fast to transfer the charge to the output. In our simulations, we used clock frequency of 300KHz. The voltage regulator consists of several diode connected nMOS transistors and is used to trim the output voltage.

The simulation results are shown in Figure 4.11. The output voltage can reach 3.3V within 200nS.

The negative substrate voltage generator is shown in Figure 4.12. When input A is high, it will charge the capacitor formed by M1 and the capacitor in series with M1 formed by the diode connected M2. Node B will be at a voltage a little higher than the threshold voltage of M2 so that M2 is operating in saturation region. M3 is in the cutoff region. When input A goes low, B will go to a negative voltage because the voltage drop across the capacitor formed by M1 can not change abruptly. At this time, M2 will be cutoff while M3 will be saturated, negative charge will be transferred to the output through the diode connected transistor M3. After some cycles, the output will reach a

المنارة للاستشارات
www.manaraa.com

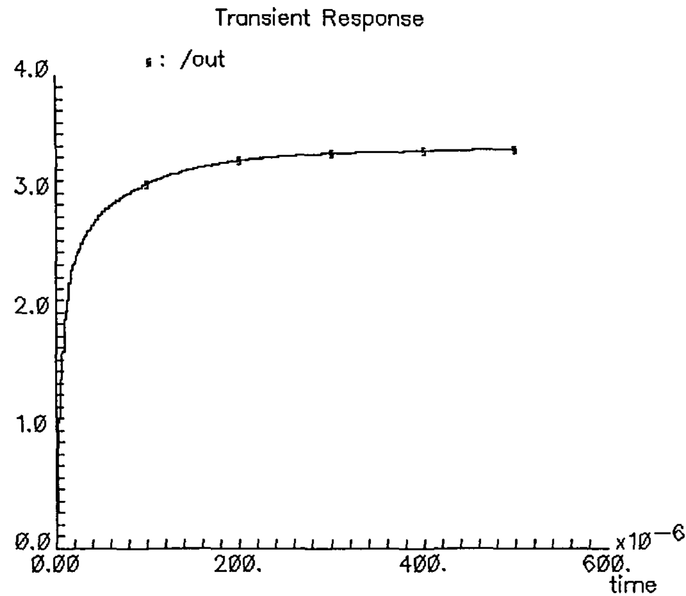

Figure 4.11 Simulation results for the charge pump

constant negative voltage. Since the input clock voltage level is only from 0 to 1.5V, using normal nMOS transistors can't generate sufficient negative voltage, floating gate MOS transistors will be used here. The floating gate MOS transistor can have a lower threshold voltage than the regular transistors. The floating gate MOSFETs used here are parasitic-type devices available in any standard process that has double polysilicon layers. More detailed characteristics about the floating gate MOSFET will be discussed in the following section.

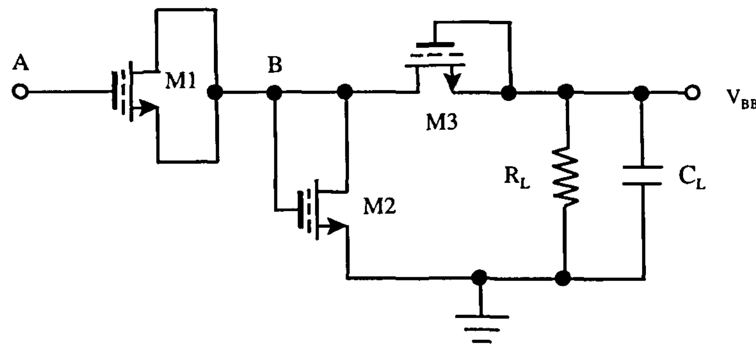

Figure 4.12 Negative substrate voltage generator

www.manaraa.com

The simulation results for the negative voltage generator are shown in Figure 4.13. It indicates that the negative voltage generator can generate -1.2V supply voltage. This negative supply voltage is sufficient to guarantee the bulk-source junction of the pass transistor in the switched capacitor circuit used to generate V_{DC} is reverse biased.

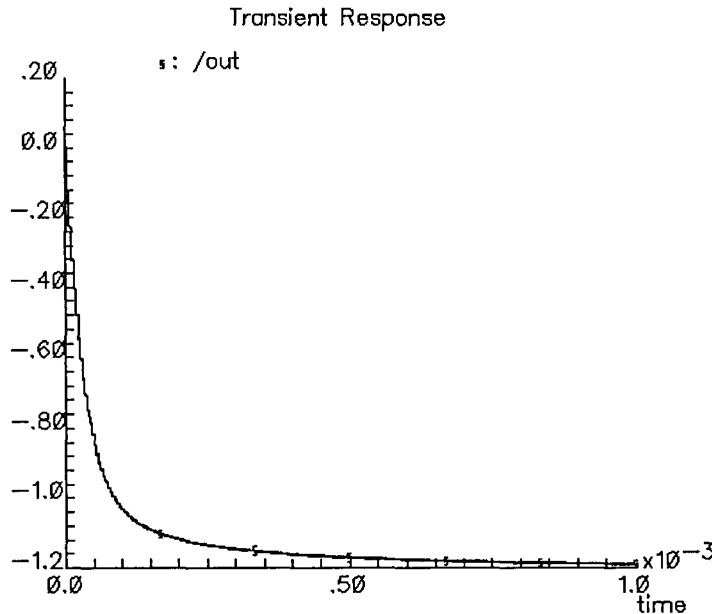

Figure 4.13 Simulation results for the negative voltage generator

4.4 Oscillator

The oscillator provides clock signals for the switched capacitors circuits, charge pump circuits, and the negative supply voltage generator discussed in the previous chapters and sections. The oscillator is realized by ring oscillator with an additional R-C delay component as shown in Figure 4.14.

The ring oscillator consists of 5 inverter stages. In order to have a 300KHz oscillation frequency, the R-C delay component was inserted among the stages. This delay component will basically determine the oscillation frequency. The power supply voltage voltage for this oscillator is only 500mV. Floating gate MOSFETs have been used for the oscillator. These are necessary to get the oscillator to start up. The effective V_T of the floating gate transistors is set to the appropriate value during initial testing. Since

www.manaraa.com

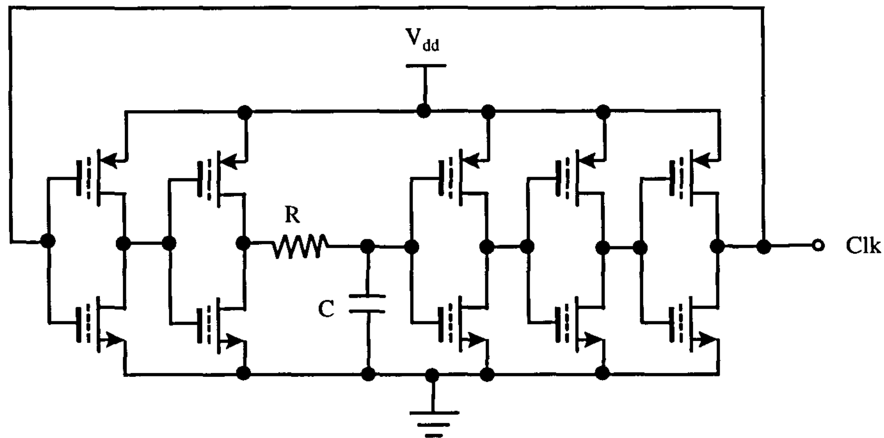

Figure 4.14 Ring oscillator

the floating gate are nonvolatile, they thus retain the charge after they are removed from the tester.

Floating-Gate devices are widely used in nonvolatile memories and analog trimming circuits [CA89] [SG88]. Figure 4.15 shows a cross section and top view of a parasitic floating gate transistor available in standard double poly CMOS processes. The first polysilicon layer is used for the floating gate. The second polysilicon layer serves as the control electrode and as the gate of all CMOS transistors used in the circuit. The write operation is done during initial circuit testing. In the write operation, the floating gate is charged with electrons tunneling along the edges of poly-I under poly-II, where tunneling distance is reduced due to the thinning of the gate oxide associated with the step along the edge of the Poly I layer. In the normal mode of operation, the floating gate can be modeled by the circuit shown in Figure 4.16.

In this model C_{sub} is the capacitance between the floating gate and the substrate, C_{ov} is the overlapping capacitance between poly-I and poly-II, C_g is the capacitance between the floating gate and the active region. The capacitance Cg is distributed and the lower plate has a distributed voltage that represents the voltage along the channel. This distributed channel voltage is often approximated to be the voltage at the source of the transistor. Q_{G1} is stored charge on the floating gate. V_{G2} can be expressed for an

www.manaraa.com

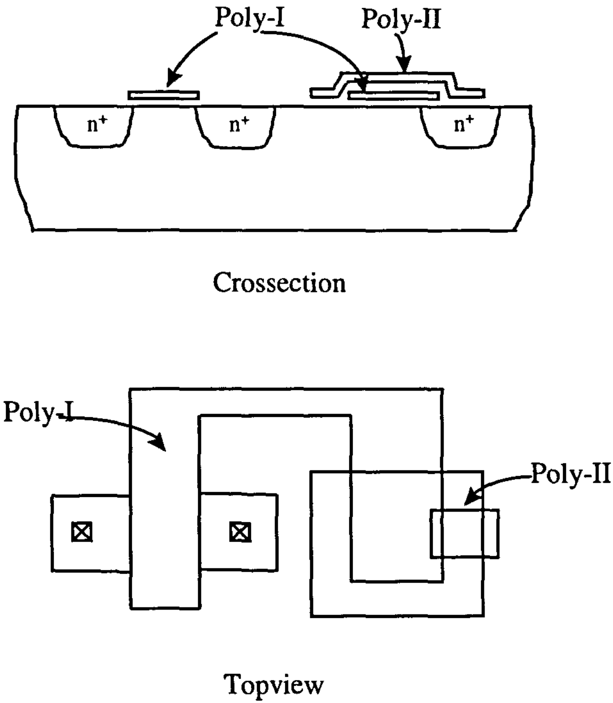

Figure 4.15 Cross section and top view of the floating gate

electrically neutral floating gate in terms of simple coupling ratios.

$$V_{G1} = \frac{C_{ov}}{C_T} \cdot V_{G2} + \frac{C_g}{C_T} \cdot V_{ch} + \frac{C_{sub}}{C_T} + \frac{Q_{G1}}{C_T} \qquad (4.24)$$

where $C_T = C_{ov} + C_g + C_{sub}$

If the overlapping capacitance C_{ov} is much larger than the sum of C_g and C_{sub}, equation (4.15) can be simplified to

$$V_{G1} \approx V_{G2} + \frac{Q_{G1}}{C_T} \qquad (4.25)$$

It thus follows from (4.25) that the stored charge shifts the threshold voltage by the value of

$$\Delta V_t = \frac{Q_{G1}}{C_T} \qquad (4.26)$$

المنارة للاستشارات
www.manaraa.com

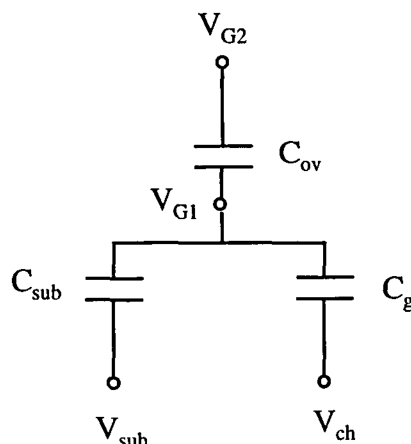

Figure 4.16 A simplified capacitive equivalent circuit of the floating gate transistor

Depending upon the polarity of the voltage placed on the floating gate, the threshold voltage shift can be either positive or negative. The output clock signal voltage of the oscillator is only 500mV which is not enough to drive the switched capacitors and charge pump circuit. The bootstrapped buffer as shown in Figure 4.17 is used to boost the output clock signal voltages to the desired level [LK97].

The principle of operation of the bootstrapped buffer can be explained as follow: When the input is low, A is high, so that M2 is off and M3 is on. The power supply will charge the capacitor C through M3 and hence B will go high. Since A is high, it will pull the output to ground. When the input goes high, A will be low, M3 will be turned off, M2 will be turned on and M1 will be turned off. Since the voltage drop on the capacitor will not change abruptly, B will go up with the input by the same amount, i.e. B will go up to $2V_{DD}$. This voltage will be transferred to the output by M2, thus the output will have voltage swing from 0 to $2V_{DD}$.

However, as can be seen from Figure 4.17, when B goes to $2V_{DD}$, M3 will be saturated, the charge on the capacitor will be discharged through M3 until B reaches $V_{DD} + V_{Tt}$. It means the boost-ratio will be degraded. But since when B approaches $V_{DD} + V_T$, the discharging current will be small. If the proper clock frequency is chosen, a reasonable boost-ratio can also be obtained. In our case, four boost stages are cascaded to

المنارة للاستشارات
www.manaraa.com

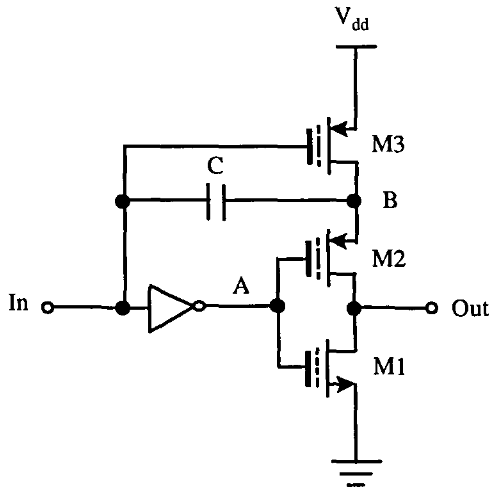

Figure 4.17 Circuit configuration of the bootstrapped buffer

boost the output level beyond what is achievable with a single boost stage. Simulation results are shown in Figure 4.18.

In Figure 4.18, /net44 represents the input to the bootstrapped circuit. The output swings from 0 to about 1.8V. The voltage drop on the output when the output clock is initially high indicates the discharging effect discussed above. This decay does not adversely affect the performance of the charge pump that this circuit drives.

4.5 Nonoverlapping clocks

Nonoverlapping clocks are used both in the switched capacitor circuits and the charge pump circuits. Nonoverlapping clocks refer to two clocks which have the same frequency while at no time both of the signals are high [JM97]. Figure 4.19 shows the nonoverlapping clocks and one method used to generate the clocks.

The delay cells in Figure 4.19 (b) are used to ensure that the clocks remain nonoverlapping. The two phases clocks ϕ_1 and ϕ_2 are sent to the bootstrapped buffer to generate two phases clocks which have voltage levels from 0V to 1.5V and are used in the charge pump circuit.

المنارة للاستشارات
www.manaraa.com

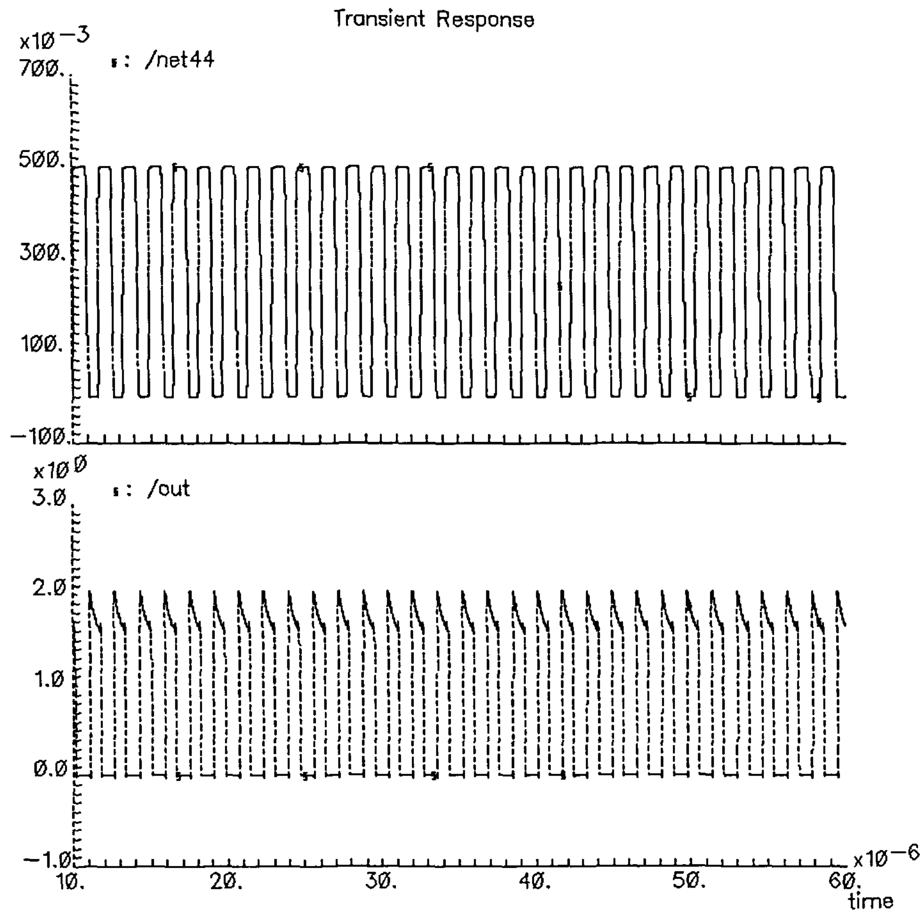

Figure 4.18 Simulation results of the bootstrapped buffer

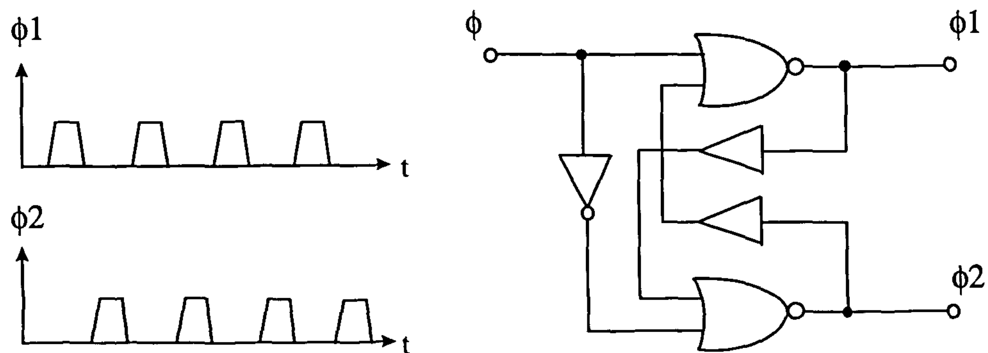

Figure 4.19 Nonoverlapping clock

(a) Clock signals (b) Circuit implementation

المنارة للاستشارات

www.manaraa.com

4.6 Pulse generator

As mentioned in the previous chapter, switched capacitors only need to be charged for a short time periodically by the waveform shown in Figure 3.10. A ring oscillator is used to generate the pulse as shown in Figure 4.20.

When power is turned on, the shift register is initialized to "000...010...000". With the shift operation continuing, the clock is divided by the shift register length and the pulse waveform is generated.

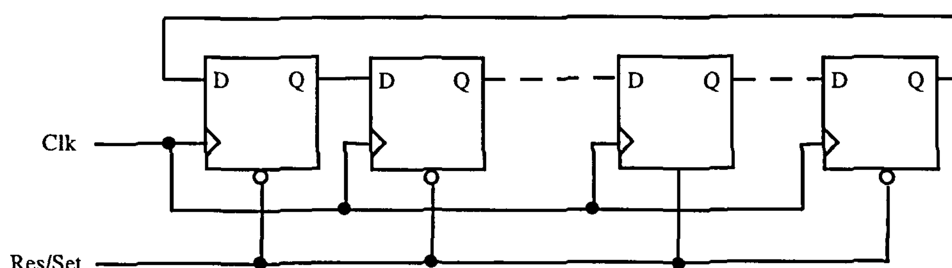

Figure 4.20 Shift register as a pulse generator

4.7 Conclusions

In this chapter, supplementary circuits such as a threshold voltage extraction circuits, an attenuator, an oscillator and a nonoverlapping clock generator were discussed. With the threshold voltage self compensation technique, threshold voltage variations due to the process and temperature variations can be eliminated. By using the on-chip floating gate oscillator, the proposed 500mV low-voltage amplifier can be realized using single 500mV power supply.

The entire operational amplifier system of Figure 4.1 including all of the supplementary circuits was simulated. The device sizes used for the supplementary circuits appear in the netlist files for the circuit simulation in Appendix C.

Although this structure will maintain a low voltage, many low voltage applications require low power as well. Full benefit of this structure will be realized when the total power dissipated in the supplementary circuits is small compared to the power

www.manaraa.com

dissipated in the operational amplifier itself. Table 4.1 shows the power dissipation in low-voltage operational amplifier circuits. It indicates that the low-voltage operational amplifier core dissipates much more power than the supplementary circuit. It is worth mention that when the analog circuit core becomes larger and larger, the power dissipated in the supplementary circuits becomes less and less in the total power dissipation in the system.

Table 4.1 Power dissipation in the low-voltage operational amplifier circuits

	Power	Percentage
Operational amplifier core	35μW	97.1
Threshold voltage extracion	0.3μW	0.83
Attenuators	0.5μW	1.39
Charge pump	0.005μW	
Ring oscillator	0.045μW	0.13
Bootstrapped buffer	0.105μW	0.3
Nonoverlapping clock	0.01μW	
Pulse generator	0.08μW	

www.manaraa.com

CHAPTER 5. CONCLUSIONS

A new method for designing ultra-low-voltage integrated circuits in a standard CMOS process was introduced. As a proof of concept vehicle, an ultra-low-voltage operational amplifier was introduced.

Simulation results indicated that by lowering the effective threshold voltage, a power supply voltage of 500mV for an operational amplifier can be used while still maintaining comparable key performance parameters to the standard 3.3V operational amplifier. The operational amplifier presented achieved a 68dB DC gain, 7.8MHz unit-gain bandwidth with a 65° phase margin compared to a 75dB DC gain, 10MHz unit-gain bandwidth with a 60° phase margin for essentially the same amplifier designed to operate with a standard 3.3V supply voltage.

To help place this work in perspective, there was considerable work on reducing supply voltages to the 5V range in the mid-to-late 1980's. In the early 90's, linear circuits that operated with 3.5V supplies started to appear with limited success with operation at the 2V level. A small number of researchers have targeted the 1V barrier with 100mV power supply voltage reductions being viewed as substantial. These low-voltage circuits often require very specialized processed. This work represents nearly a factor of 2 reduction in supply voltage down to the 500mV level while still using a standard commercial CMOS process.

Although the focus in this thesis has been on maintaining performance parameters comparable to those achievable with larger supply voltages and larger power dissipation, it should be emphasized that the dominant applications of this technique will be for very low-voltage systems. In these cases, substantial further decreases in power dissipation can be attained paralleling a deterioration in amplifier bandwidth. This technique can also be

www.manaraa.com

used for designing a variety of other analog and mixed-signal systems that operate at very low-voltages and with low power levels.

المنارة للاستشارات

www.manaraa.com

APPENDIX A. LEVEL 3 HSPICE MODEL

```
.MODEL CMOSN NMOS
LEVEL=3 PHI=0.700000 TOX=9.6000E-09 XJ=0.200000U TPG=1
+ VTO=0.6566 DELTA=6.9100E-01 LD=4.7290E-08 KP=1.9647E-04
+ UO=546.2 THETA=2.6840E-01 RSH=3.5120E+01 GAMMA=0.5976
+ NSUB=1.3920E+17 NFS=5.9090E+11 VMAX=2.0080E+05 ETA=3.7180E-02
+ KAPPA=2.8980E-02 CGDO=3.0515E-10 CGSO=3.0515E-10
+ CGBO=4.0239E-10 CJ=5.62E-04 MJ=0.559 CJSW=5.00E-11
+ MJSW=0.521 PB=0.99
* Weff = Wdrawn - Delta_W
* The suggested Delta_W is 4.1080E-07
.MODEL CMOSP PMOS
LEVEL=3 PHI=0.700000 TOX=9.6000E-09 XJ=0.200000U TPG=-1
+ VTO=-0.9213 DELTA=2.8750E-01 LD=3.5070E-08 KP=4.8740E-05
+ UO=135.5 THETA=1.8070E-01 RSH=1.1000E-01 GAMMA=0.4673
+ NSUB=8.5120E+16 NFS=6.5000E+11 VMAX=2.5420E+05 ETA=2.4500E-02
+ KAPPA=7.9580E+00 CGDO=2.3922E-10 CGSO=2.3922E-10
+ CGBO=3.7579E-10 CJ=9.35E-04 MJ=0.468 CJSW=2.89E-10
+ MJSW=0.505 PB=0.99
* Weff = Wdrawn - Delta_W
* The suggested Delta_W is 3.6220E-07
```

www.manaraa.com

APPENDIX B. LEVEL 13 HSPICE MODEL

```
*PROCESS=HP
*RUN=n5bo
*WAFER=42
*Gate-oxide thickness= 96 angstroms
*DATE=1-Feb-1996
*
*NMOS PARAMETERS
*
-7.05628E-01,-3.86432E-02, 4.98790E-02
 8.41845E-01, 0.00000E+00, 0.00000E+00
 7.76570E-01,-7.65089E-04,-4.83494E-02
 2.66993E-02, 4.57480E-02,-2.58917E-02
-1.94480E-03, 1.74351E-02,-5.08914E-03
 5.75297E+02,1.70587E-001,4.75746E-001
 3.30513E-01, 9.75110E-02,-8.58678E-02
 3.26384E-02, 2.94349E-02,-1.38002E-02
 9.73293E+00,-5.62944E+00, 6.55955E+00
 4.37180E-04,-3.07010E-03, 8.94355E-04
-5.05012E-05,-1.68530E-03,-1.42701E-03
-1.11542E-02,-9.58423E-04, 4.61645E-03
-1.04401E-03, 1.29001E-03,-7.10095E-04
 6.92716E+02,-5.21760E+01, 7.00912E+00
-6.41307E-02, 1.37809E+00, 4.15455E+00
 8.86387E+00, 2.06021E+00,-6.19817E+00
 9.02467E-03, 2.06380E-04,-5.20218E-03
9.60000E-003, 2.70000E+01, 5.00000E+00
3.60204E-010,3.60204E-010,4.37925E-010
1.00000E+000,0.00000E+000,0.00000E+000
1.00000E+000,0.00000E+000,0.00000E+000
0.00000E+000,0.00000E+000,0.00000E+000
0.00000E+000,0.00000E+000,0.00000E+000
*
* Gate Oxide Thickness is 96 Angstroms
*
*
*PMOS PARAMETERS
```

www.manaraa.com

```
*
-2.02610E-01, 3.59493E-02,-1.10651E-01
 8.25364E-01, 0.00000E+00, 0.00000E+00
 3.54162E-01,-6.88193E-02, 1.52476E-01
-4.51065E-02, 9.41324E-03, 3.52243E-02
-1.07507E-02, 1.96344E-02,-3.51067E-04
 1.37992E+02,1.92169E-001,4.68470E-001
 1.89331E-01, 6.30898E-02,-6.38388E-02
 1.31710E-02, 1.44096E-02, 6.92372E-04
 6.57709E+00,-1.56096E+00, 1.13564E+00
 4.68478E-05,-1.09352E-03,-1.53111E-04
 7.76679E-04,-1.97213E-04,-1.12034E-03
 8.71439E-03,-1.92306E-03, 1.86243E-03
 5.98941E-04, 4.54922E-04, 3.11794E-04
 1.49460E+02, 1.36152E+01, 3.55246E+00
 6.37235E+00,-6.63305E-01, 2.25929E+00
-1.21135E-02, 1.92973E+00, 1.00182E+00
-1.16599E-03,-5.08278E-04, 9.56791E-04
9.60000E-003, 2.70000E+01, 5.00000E+00
4.18427E-010,4.18427E-010,4.33943E-010
1.00000E+000,0.00000E+000,0.00000E+000
1.00000E+000,0.00000E+000,0.00000E+000
0.00000E+000,0.00000E+000,0.00000E+000
0.00000E+000,0.00000E+000,0.00000E+000
*
*N+ diffusion::
*
2.1,   3.500000e-04,   2.900000e-10,   1e-08,   0.8
0.8,   0.44,   0.26,   0,   0
*
*P+ diffusion::
*
2,   9.452900e-04,   2.458300e-10,   1e-08,   0.85
0.85,   0.439735,   0.237251,   0,   0
*
*METAL LAYER -- 1
*
0.07,   2.6e-05,   0,   0,   0
0,   0,   0,   0,   0
*
*METAL LAYER -- 2
*
0.07,   1.3e-05,   0,   0,   0
0,   0,   0,   0,   0
```

المنارة للاستشارات
www.manaraa.com

APPENDIX C: NETLIST FOR THE CIRCUIT SIMULATION

a). Netlist for operational amplifier core

```
* netlist/opamprc.c.raw
XI39 NET12 NET41 SUB1
XI40 NET12 NET24 SUB1
XI41 NET67 NET28 SUB1
XI38 NET19 NET53 SUB2
XI37 NET21 NET35 SUB2
XI35 NET63 NET27 SUB2
XI36 NET21 NET25 SUB2
R31 NET67 NET98  12E3 M=1.0
C29 NET98 OUT  2E-12 M=1.0
C27 OUT 0  5E-12 M=1.0
V43 NET63 0  380E-3 AC 1.0
V44 NET19 0  380E-3
V16 G2 0  500E-3 AC 0.0
V12 NET21 0  300E-3
M24 OUT NET28 G2 G2  CMOSP  L=2.1E-6 W=398E-6 AD=450E-12 AS=450E-12
PD=300E-6
+PS=300E-6 M=1.0
M15 NET12 NET41 G2 G2  CMOSP  L=2.1E-6 W=80E-6 AD=60E-12 AS=60E-12
PD=40E-6
+PS=40E-6 M=1.0
M4 NET67 NET24 G2 G2  CMOSP  L=2.1E-6 W=80E-6 AD=60E-12 AS=60E-12
PD=40E-6
+PS=40E-6 M=1.0
M26 OUT NET25 0 0  CMOSN  L=2.1E-6 W=48E-6 AD=80E-12 AS=80E-12 PD=50E-
6
+PS=50E-6 M=1.0
M6 NET12 NET27 NET83 0  CMOSN  L=2.1E-6 W=20E-6 AD=15E-12 AS=15E-12
PD=15E-6
+PS=15E-6 M=1.0
M14 NET67 NET53 NET83 0  CMOSN  L=2.1E-6 W=20E-6 AD=15E-12 AS=15E-12
PD=15E-6
+PS=15E-6 M=1.0
M0 NET83 NET35 0 0  CMOSN  L=2.1E-6 W=20E-6 AD=30E-12 AS=30E-12
PD=25E-6
```

www.manaraa.com

```
+PS=25E-6 M=1.0

.SUBCKT SUB1 IN OUT
V11 NET14 OUT  800E-3
R10 IN NET14  100E9 M=1.0
C13 0 IN  1E-15 M=1.0
C7 0 OUT  1E-15 M=1.0
C0 IN OUT  10E-12 M=1.0
.ENDS SUB1

.SUBCKT SUB2 IN OUT
V11 OUT NET14  670E-3
R10 IN NET14  10E9 M=1.0
C13 0 IN  1E-15 M=1.0
C7 0 OUT  1E-15 M=1.0
C0 IN OUT  100E-12 M=1.0
.ENDS SUB2

.AC DEC     10.0000     1.00000     1.000000E+10
.TEMP    25.0000
.OP
.save
.OPTION  INGOLD=2 ARTIST=2 PSF=2
+       PROBE=0
+       LIST
+       ACOUT  =  .00000E+00
.END
```

www.manaraa.com

b). Netlist for reference voltage generation circuits

```
* Threshold.c.raw
.GLOBAL G1
XI17 NET10 V3 SUB1
XI16 G1 V4 SUB1
XI15 0 V1 SUB2
XI14 NET44 V2 SUB2
V8 G1 0  3.3
M5 NET10 NET10 G1 G1  CMOSP  L=6E-6 W=24E-6 AD=36E-12 AS=36E-12
PD=50E-6
+PS=50E-6 M=1.0
M13 NET10 G1 NET44 0  CMOSN  L=180E-6 W=900E-9 AD=2E-12 AS=2E-12
PD=4.8E-6
+PS=4.8E-6 M=1.0
M1 NET44 NET44 0 0  CMOSN  L=6E-6 W=6E-6 AD=9E-12 AS=9E-12 PD=15E-6
PS=15E-6
+M=1.0

.SUBCKT SUB1 IN OUT
M5 G1 IN OUT 0  CMOSN  L=6E-6 W=6E-6 AD=9E-12 AS=0.0 PD=15E-6 PS=15E-6
M=1.0
M0 OUT IN 0 0  CMOSN  L=178E-6 W=900E-9 AD=2E-12 AS=2E-12 PD=4.8E-6
PS=4.8E-6
+M=1.0
.ENDS SUB1

.SUBCKT SUB2 IN OUT
M14 OUT IN G1 G1  CMOSP  L=178E-6 W=900E-9 AD=2E-12 AS=2E-12 PD=4.8E-6
+PS=4.8E-6 M=1.0
M15 0 IN OUT G1  CMOSP  L=6E-6 W=6E-6 AD=9E-12 AS=9E-12 PD=15E-6
PS=15E-6
+M=1.0
.ENDS SUB2


.TEMP    25.0000
.OP
.save
.OPTION  INGOLD=2 ARTIST=2 PSF=2
```

www.manaraa.com

```
+       PROBE=0
+       LIST
+       ACOUT  =  .00000E+00
.END
```

المنارة للاستشارات
www.manaraa.com

c). Netlist for oscillator and bootstrapping circuits

```
* netlist/osc.c.raw
.GLOBAL G1
V22 G1 0  500E-3
R20 NET55 NET50  100E3 M=1.0
C101 NET198 NET153  10E-12 M=1.0
C84 NET94 NET61  10E-12 M=1.0
C118 NET114 NET65  10E-12 M=1.0
C83 NET106 NET133  10E-12 M=1.0
C19 NET50 0  10E-12 IC=1.0 M=1.0
M103 OUT NET161 0 0  CMOSN  L=2E-6 W=10E-6 AD=4.5E-12 AS=4.5E-12 PD=6E-
6
+PS=6E-6 M=1.0
M37 NET153 NET161 0 0  CMOSN  L=2E-6 W=10E-6 AD=4.5E-12 AS=4.5E-12
PD=6E-6
+PS=6E-6 M=1.0
M94 NET131 NET44 0 0  CMOSN  L=2E-6 W=6E-6 AD=4.5E-12 AS=4.5E-12 PD=6E-
6
+PS=6E-6 M=1.0
M99 NET161 NET131 0 0  CMOSN  L=2E-6 W=18E-6 AD=4.5E-12 AS=4.5E-12
PD=6E-6
+PS=6E-6 M=1.0
M96 NET133 NET161 0 0  CMOSN  L=2E-6 W=40E-6 AD=4.5E-12 AS=4.5E-12
PD=6E-6
+PS=6E-6 M=1.0
M97 NET61 NET161 0 0  CMOSN  L=2E-6 W=10E-6 AD=4.5E-12 AS=4.5E-12
PD=6E-6
+PS=6E-6 M=1.0
M36 NET65 NET161 0 0  CMOSN  L=2E-6 W=10E-6 AD=4.5E-12 AS=4.5E-12
PD=6E-6
+PS=6E-6 M=1.0
M124 NET44 NET40 0 0  CMOSN  L=2E-6 W=3E-6 AD=4.5E-12 AS=4.5E-12 PD=6E-
6
+PS=6E-6 M=1.0
M127 NET55 NET59 0 0  CMOSN  L=2E-6 W=3E-6 AD=4.5E-12 AS=4.5E-12 PD=6E-
6
+PS=6E-6 M=1.0
M125 NET10 NET44 0 0  CMOSN  L=2E-6 W=3E-6 AD=4.5E-12 AS=4.5E-12 PD=6E-
6
```

المنارة للاستشارات
www.manaraa.com

```
+PS=6E-6 M=1.0
M73 NET40 NET50 0 0  CMOSN  L=2E-6 W=3E-6 AD=4.5E-12 AS=4.5E-12 PD=6E-6
+PS=6E-6 M=1.0
M126 NET59 NET10 0 0  CMOSN  L=2E-6 W=3E-6 AD=4.5E-12 AS=4.5E-12 PD=6E-
6
+PS=6E-6 M=1.0
M122 NET59 NET10 G1 G1  CMOSP  L=2E-6 W=6E-6 AD=12E-12 AS=12E-12
PD=10E-6
+PS=10E-6 M=1.0
M121 NET10 NET44 G1 G1  CMOSP  L=2E-6 W=6E-6 AD=12E-12 AS=12E-12
PD=10E-6
+PS=10E-6 M=1.0
M120 NET44 NET40 G1 G1  CMOSP  L=2E-6 W=6E-6 AD=12E-12 AS=12E-12
PD=10E-6
+PS=10E-6 M=1.0
M111 G1 NET153 NET198 NET198  CMOSP  L=2E-6 W=5E-6 AD=12E-12 AS=12E-
12
+PD=10E-6 PS=10E-6 M=1.0
M98 NET131 NET44 G1 G1  CMOSP  L=2E-6 W=15E-6 AD=12E-12 AS=12E-12
PD=10E-6
+PS=10E-6 M=1.0
M69 NET40 NET50 G1 G1  CMOSP  L=2E-6 W=6E-6 AD=12E-12 AS=12E-12
PD=10E-6
+PS=10E-6 M=1.0
M105 OUT NET161 NET198 NET198  CMOSP  L=2E-6 W=30E-6 AD=4.5E-12
AS=4.5E-12
+PD=8E-6 PS=8E-6 M=1.0
M92 G1 NET133 NET106 NET106  CMOSP  L=2E-6 W=3E-6 AD=12E-12 AS=12E-12
PD=10E-6
+PS=10E-6 M=1.0
M34 NET65 NET161 NET94 NET94  CMOSP  L=2E-6 W=30E-6 AD=4.5E-12
AS=4.5E-12
+PD=8E-6 PS=8E-6 M=1.0
M35 NET153 NET161 NET114 NET114  CMOSP  L=2E-6 W=30E-6 AD=4.5E-12
AS=4.5E-12
+PD=8E-6 PS=8E-6 M=1.0
M91 NET133 NET161 G1 G1  CMOSP  L=2E-6 W=60E-6 AD=12E-12 AS=12E-12
PD=10E-6
+PS=10E-6 M=1.0
M93 NET61 NET161 NET106 NET106  CMOSP  L=2E-6 W=30E-6 AD=4.5E-12
AS=4.5E-12
+PD=8E-6 PS=8E-6 M=1.0
M109 G1 NET61 NET94 NET94  CMOSP  L=2E-6 W=5E-6 AD=12E-12 AS=12E-12
PD=10E-6
```

المنارة للاستشارات
www.manaraa.com

```
+PS=10E-6 M=1.0
M110 G1 NET65 NET114 NET114  CMOSP  L=2E-6 W=5E-6 AD=12E-12 AS=12E-12
PD=10E-6
+PS=10E-6 M=1.0
M123 NET55 NET59 G1 G1  CMOSP  L=2E-6 W=6E-6 AD=12E-12 AS=12E-12
PD=10E-6
+PS=10E-6 M=1.0
M85 NET161 NET131 G1 G1  CMOSP  L=2E-6 W=30E-6 AD=12E-12 AS=12E-12
PD=10E-6
+PS=10E-6 M=1.0

.AC DEC      10.0000      1.00000      1.000000E+10
.TEMP    25.0000
.OP
.save
.OPTION  INGOLD=2 ARTIST=2 PSF=2
+       PROBE=0
+       LIST
+       ACOUT  =  .00000E+00
.END
```

المنارة للاستشارات
www.manaraa.com

d). Netlist for the charge pump circuit

```
 * cp.c.raw
M131 NET220 PH1 NET133 G1  CMOSP  L=900E-9 W=6E-6 AD=9E-12 AS=9E-12
PD=15E-6
+PS=15E-6 M=1.0
M130 NET219 PH1 NET125 G1  CMOSP  L=900E-9 W=6E-6 AD=9E-12 AS=9E-12
PD=15E-6
+PS=15E-6 M=1.0
M129 NET36 PH1 NET157 G1  CMOSP  L=900E-9 W=6E-6 AD=9E-12 AS=9E-12
PD=15E-6
+PS=15E-6 M=1.0
M128 NET38 PH1 NET71 G1  CMOSP  L=900E-9 W=6E-6 AD=9E-12 AS=9E-12
PD=15E-6
+PS=15E-6 M=1.0
M127 NET42 PH1 NET75 G1  CMOSP  L=900E-9 W=6E-6 AD=9E-12 AS=9E-12
PD=15E-6
+PS=15E-6 M=1.0
M126 NET40 PH1 NET91 G1  CMOSP  L=900E-9 W=6E-6 AD=9E-12 AS=9E-12
PD=15E-6
+PS=15E-6 M=1.0
M125 NET44 PH1 NET87 G1  CMOSP  L=900E-9 W=6E-6 AD=9E-12 AS=9E-12
PD=15E-6
+PS=15E-6 M=1.0
M124 NET46 PH1 NET103 G1  CMOSP  L=900E-9 W=6E-6 AD=9E-12 AS=9E-12
PD=15E-6
+PS=15E-6 M=1.0
C106 NET219 NET157  100E-12 M=1.0
C110 NET220 NET125  100E-12 M=1.0
C74 NET36 NET71  100E-12 M=1.0
C35 OUT 0  10E-12 IC=0.0 M=1.0
C65 NET38 NET75  100E-12 M=1.0
C64 NET42 NET91  100E-12 M=1.0
C62 NET44 NET103  100E-12 M=1.0
C63 NET40 NET87  100E-12 M=1.0
C7 NET46 0  100E-12 M=1.0
M111 G1 PH2 NET220 0  CMOSN  L=2E-6 W=3E-6 AD=4.5E-12 AS=4.5E-12 PD=8E-
6
+PS=8E-6 M=1.0
```

المنارة للاستشارات

www.manaraa.com

M107 G1 PH2 NET219 0 CMOSN L=2E-6 W=3E-6 AD=4.5E-12 AS=4.5E-12 PD=8E-
6
+PS=8E-6 M=1.0
M108 NET157 PH2 0 0 CMOSN L=2E-6 W=3E-6 AD=4.5E-12 AS=4.5E-12 PD=8E-6
+PS=8E-6 M=1.0
M112 NET125 PH2 0 0 CMOSN L=2E-6 W=3E-6 AD=4.5E-12 AS=4.5E-12 PD=8E-6
+PS=8E-6 M=1.0
M117 NET279 NET279 NET275 0 CMOSN L=2E-6 W=3E-6 AD=4.5E-12 AS=4.5E-
12
+PD=8E-6 PS=8E-6 M=1.0
M118 NET275 NET275 NET287 0 CMOSN L=2E-6 W=3E-6 AD=4.5E-12 AS=4.5E-
12
+PD=8E-6 PS=8E-6 M=1.0
M119 NET287 NET287 0 0 CMOSN L=2E-6 W=3E-6 AD=4.5E-12 AS=4.5E-12
PD=8E-6
+PS=8E-6 M=1.0
M120 OUT OUT NET279 0 CMOSN L=2E-6 W=3E-6 AD=4.5E-12 AS=4.5E-12
PD=8E-6
+PS=8E-6 M=1.0
M58 G1 PH2 NET44 0 CMOSN L=2E-6 W=3E-6 AD=4.5E-12 AS=4.5E-12 PD=8E-6
PS=8E-6
+M=1.0
M59 G1 PH2 NET40 0 CMOSN L=2E-6 W=3E-6 AD=4.5E-12 AS=4.5E-12 PD=8E-6
PS=8E-6
+M=1.0
M71 G1 PH2 NET36 0 CMOSN L=2E-6 W=3E-6 AD=4.5E-12 AS=4.5E-12 PD=8E-6
PS=8E-6
+M=1.0
M60 G1 PH2 NET42 0 CMOSN L=2E-6 W=3E-6 AD=4.5E-12 AS=4.5E-12 PD=8E-6
PS=8E-6
+M=1.0
M30 NET133 NET133 OUT 0 CMOSN L=600E-9 W=3E-6 M=1.0
M70 NET71 PH2 0 0 CMOSN L=2E-6 W=3E-6 AD=4.5E-12 AS=4.5E-12 PD=8E-6
PS=8E-6
+M=1.0
M69 NET75 PH2 0 0 CMOSN L=2E-6 W=3E-6 AD=4.5E-12 AS=4.5E-12 PD=8E-6
PS=8E-6
+M=1.0
M67 NET87 PH2 0 0 CMOSN L=2E-6 W=3E-6 AD=4.5E-12 AS=4.5E-12 PD=8E-6
PS=8E-6
+M=1.0
M68 NET91 PH2 0 0 CMOSN L=2E-6 W=3E-6 AD=4.5E-12 AS=4.5E-12 PD=8E-6
PS=8E-6
+M=1.0

المنارة للاستشارات
www.manaraa.com

```
M66 NET103 PH2 0 0  CMOSN  L=2E-6 W=3E-6 AD=4.5E-12 AS=4.5E-12 PD=8E-6
PS=8E-6
+M=1.0
M61 G1 PH2 NET38 0  CMOSN  L=2E-6 W=3E-6 AD=4.5E-12 AS=4.5E-12 PD=8E-6
PS=8E-6
+M=1.0
M5 G1 PH2 NET46 0  CMOSN  L=2E-6 W=3E-6 AD=4.5E-12 AS=4.5E-12 PD=8E-6
PS=8E-6
+M=1.0
V2 G1 0  500E-3
.AC DEC      10.0000      1.00000      1.000000E+10
.TEMP    25.0000
.OP
.save
.OPTION  INGOLD=2 ARTIST=2 PSF=2
+       PROBE=0
+       LIST
+       ACOUT  =  .00000E+00
.END
```

المنارة للاستشارات

www.manaraa.com

BIBLIOGRAPHY

[AB95] Phillip E. Allen, Benjamin J. Blalock and Gabriel A. Rincon, "A 1V CMOS Opamp Using Bulk-Driven MOSFETs", IEEE Int. Solid-State Circuits Conf., pp. 192-3, 1995.

[AC95] J. Ramirez-Angulo, S. C. Choi, and G. Gonzalez-Altamirano, "Low-Voltage Circuits Building Blocks Using Multiple-Input Floating-Gate Transistors", IEEE Transactions on Circuits and System-I: Fundamental Theory and Applications, Vol. 42, No. 11, pp. 971-4, Nov. 1995.

[AH87] Phillip E. Allen and Douglas R. Holberg, CMOS Analog Circuit Design, Holt, Rinehart and Winston, New York, 1987.

[CA89] L. Richard Carley, "Trimming Analog Circuits Using Floating-Gate Analog MOS Memory", IEEE Int. Solid-State Circuits Conf., pp. 202-3, 1989.

[EC96] Jean-Paul Eggermont, Denis De Ceuster, et al., "Design of SOI CMOS Operational Amplifiers for Applications up to 300°C", IEEE J. Solid-State Circuits, Vol. 31, No. 2, pp. 179-86, Feb. 1996.

[FM89] Jeroen Fonderie, Marinus G. Maris and Johan H. Huijsing, "1-Volt Operationam Amplifier with Rail-to-Rail Input and Output Ranges", IEEE Int. Solid-State Circuits Conf., pp. 64-5, 1989.

[GA90] Randall L. Geiger, Phillip E. Allen and Neol R. Strader, VLSI Design Techniques for Analog and Digital Circuits, McGraw-Hill, New York, 1990.

[HC97] Shu-Chuan Huang and Chin-Chun Chang, "Design of a BiCMOS Constant-g_m Rail-to-Rail Operational Amplifier for Low-Voltage Applications", IEEE Intl. Symp. Circuits and Syst., Vol. 1, pp. 161-4, 1997.

[HH96] Ron Hogevorst and Johan H. Huijsing, Design of Low-Voltage, Low-Power Operational Amplifier Cells, Kluwer Academic, The Netherlands, 1996.

المنارة للاستشارات

www.manaraa.com

[HL85] Johan H. Huijsing and Daniel Linebarger, "Low-Voltage Operational Amplifier with Rail-to-Rail Input and Output Ranges", IEEE J. Solid-State Circuits, Vol. SC-20, No. 6, pp. 1144-49, Dec. 1985.

[JM97] David A. Johns and Ken Martin, Analog Integrated Circuit Design, John Wiley and Sons, New York, 1997.

[KI95] Joon-Yub Kim, Monolithic Finite Gain Amplifiers Employing Active Voltage Attenuators in the Feedback and a Charge Conserving Macromodel for MOSFETs, Ph.D dissertation, Iowa State University, 1995.

[KT96] Shigeru Kuhara, Hideo Toyoshima et al. "6nS 1.5V 4Mb BiCMOS SRAM", Proc. IEEE Inter. Solid-State Circuits Conf., pp. 104-5, 1996.

[LK97] J. H. Lou and J. B. Kuo, "A 1.5-V Full-Swing Bootstrapped CMOS Large Capacitive-Load Driver Circuit Suitable for Low-Voltage CMOS VLSI", IEEE J. Solid-State Circuits, Vol. 32, No. 1, pp. 119-21, Jan. 1997.

[MA96] Saqib Q. Malik, Design Methodology for Very Low Voltage CMOS Digital Circuits, M.S thesis, Iowa State University, 1996.

[MU96] Igor Mucha, "Low-Voltage Current Operational Amplifier with A Very Low Current Consumption", Proc. IEEE Inter. Symp. Circuits and Syst., Vol. 1, pp525-28, 1996.

[RC95] J. Ramirez-Angulo, S. C. Choi and Gonzalez-Altamirano, "Low-Voltage Circuits Building Blocks Using Multiple-Input Floating-Gate Transistors", IEEE Transactions on Circuits and Systems I: Fundamental Theory and Application, Vol. 42, No. 11, pp. 971-73, Nov, 1995.

[SG88] Eduard Sackinger and Walter Guggenbuhl, "An Analog Trimming Circuit Based on a Floating-Gate Device", IEEE J. Solid-State Circuit, Vol. 23, No. 6, pp1437-40, Dec. 1988.

[SI95] Satoshi Sakurai and Mohammed Ismail, Low-voltage CMOS Operational Amplifiers, Theory, Design and Implementation, Kluwer Academic, Boston, 1995.

المنارة للاستشارات

www.manaraa.com

[SI96] Satoshi Sakurai and Mohammed Ismail, "Robust Design of Rail-to-Rail CMOS Operational Amplifiers for a Low Power Supply Voltage", IEEE J. of Solid-State and Circuits, Vol. 31, No. 2, pp. 146-56, Feb. 1996.

[ST95] Shih-Wei Sun and Paul G. Y. Tsui, "Limitation of CMOS Supply-Voltage Scaling by MOSFET Threshold-Voltage Variation", IEEE J. of Solid-Stage Circuits, Vol. 30, No. 8, pp. 947-49, Aug. 1995.

[WE93] Neil H. E. Weste and Kamran, Eshraghian, Principle of CMOS VLSI Design, a System Perspective. Second Edition, Anderson-Wesley, New York, 1993.

[YU93] Chong-Gun Yu, A Digital Tuning Scheme for Digitally Programmable Integrated Continuous-Time Filters and Techniques for High-Precision Monolithic Linear Circuit Design and Implementation, Ph.D Dissertation, Iowa State University, 1993.

المنارة للاستشارات

www.manaraa.com